RHIC能量扫描中的超核产生测量
- Focus on the High Baryon Density Region

谢冠男 (XIE Guannan)

中国科学院大学 (UCAS)

2024/11/17

Contents

- Introduction
- STAR Experiment & Beam Energy Scan
- What have been measured on Hypernuclei from STAR
  Intrinsic Properties :
  -- Lifetime, Branch Ratios & Binding Energy
  Productions :
  -- Energy dependence and Rapidity dependence Yields/Collectivity
- What's the future proposals from worldwide facilities
  For Hypernuclei? Hyperon-nucleon?

Experimental Exploring of QCD Matters

Particle production:

- ➢ Understand medium properties and different particle production mechanisms

Collective flow:

- ➢ Study properties of the produced medium, EoS

Correlations and Criticality:

- ➢ Critical Point

Phys. Rev. Lett. 128 (2022) 202303

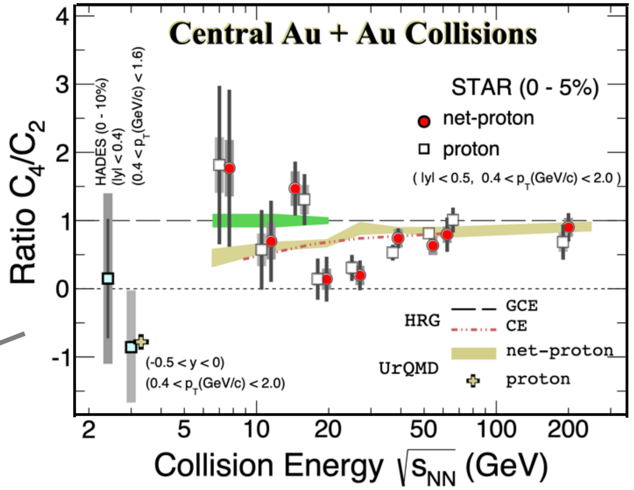

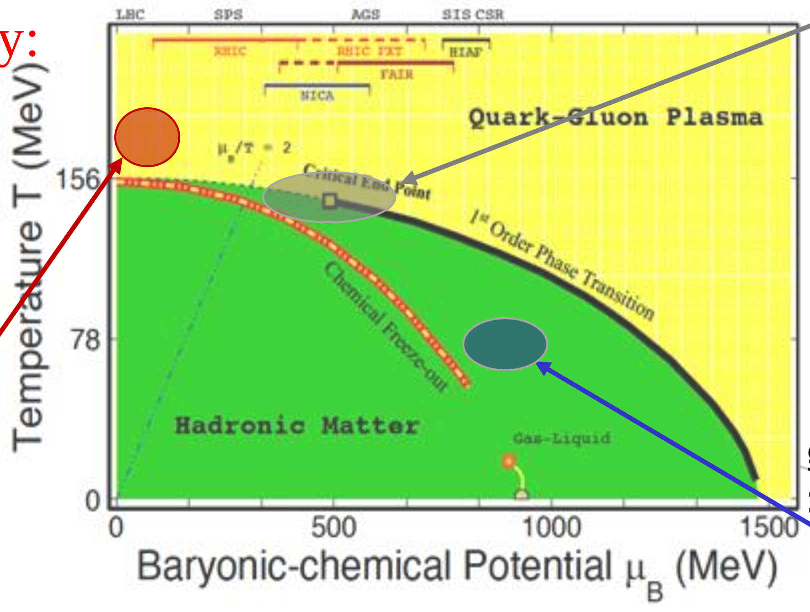

Phys. Rev. Lett. 91 (2003) 72304

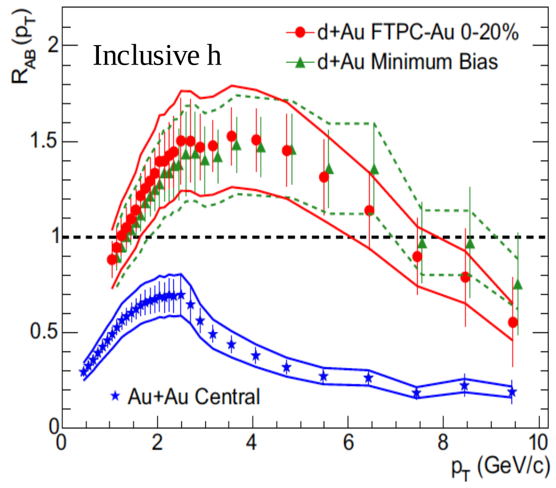

Phys. Lett. B 827 (2022) 137003

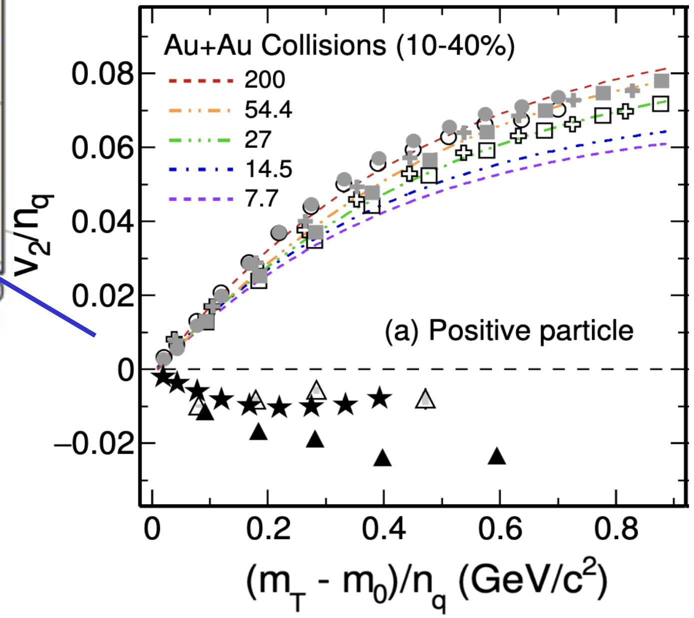

- Jet quenching, Strangeness enhancement, flow NCQ scaling, heavy flavor R_{AA}, etc
- High order Cumulants, light nuclei ratios
- NCQ disappearing, strangeness CE

HICs @ High Baryon Density Region

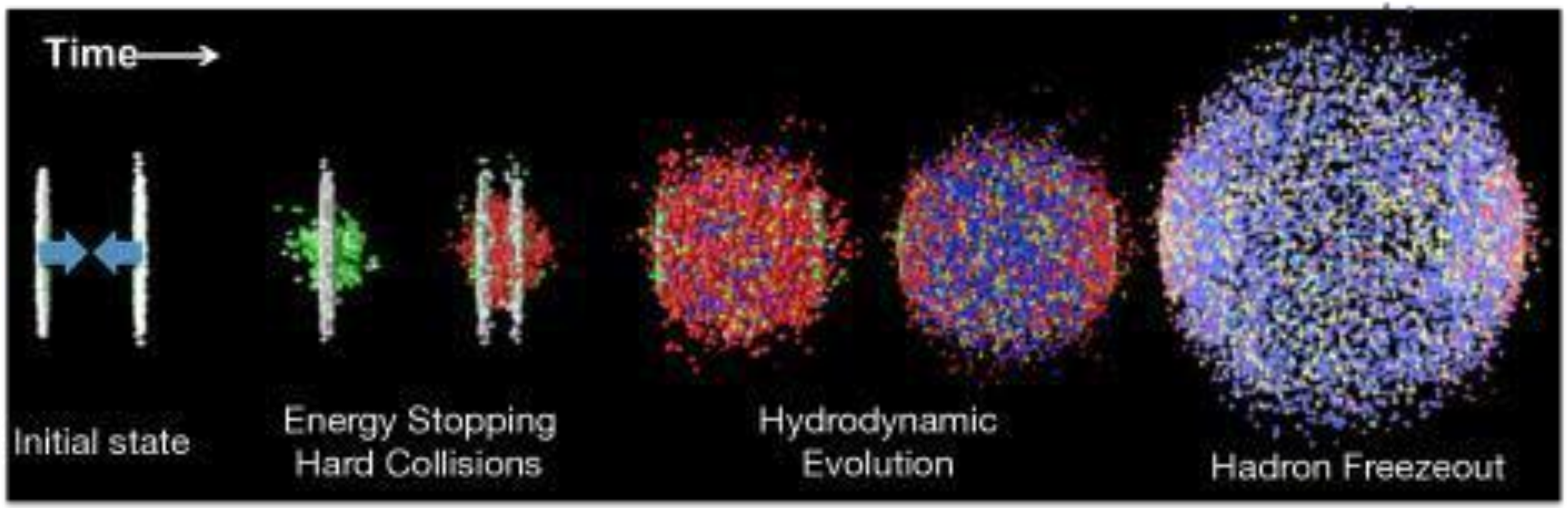

Time Evolution of HICs

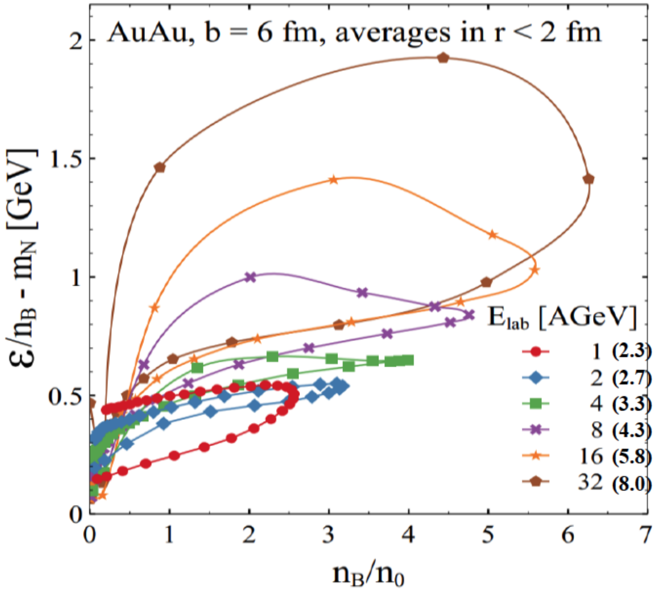

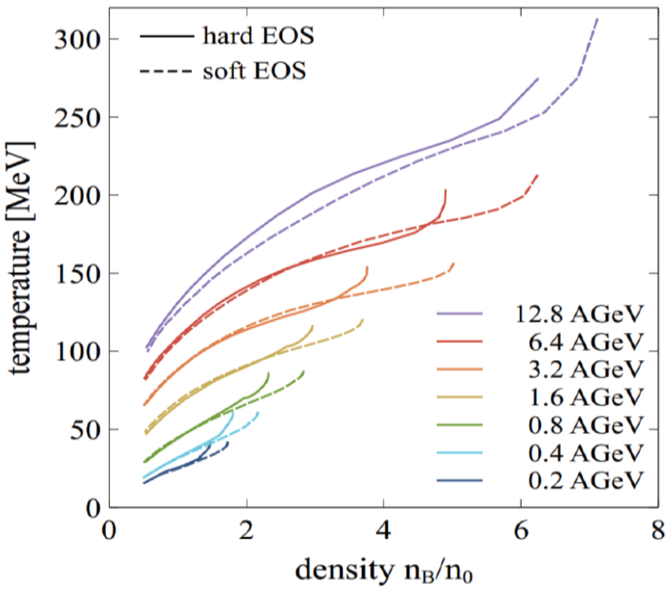

D.Oliinychenko et. al, arXiv:2208.11996 v2

A. Sorensen et. al, arXiv:2301.13253v2

Hypernuclei (What)

Nuclei are loosely bound objects with binding energies of few MeV
Hypernuclei are nuclei containing at least one hyperon (Y)
- N/Z + additional dimension on strangeness

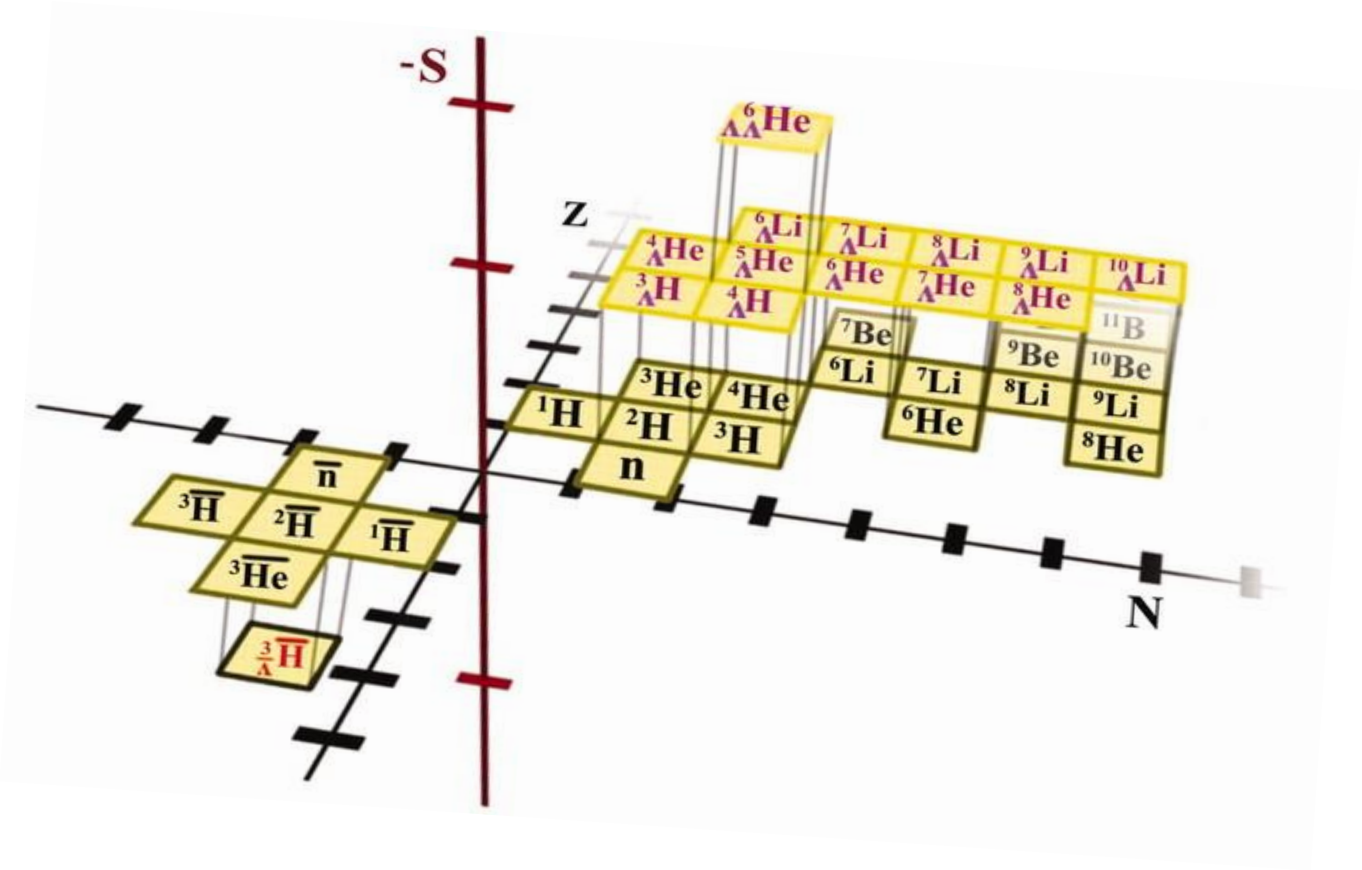

Figure from Science 328 (2010) 58-62

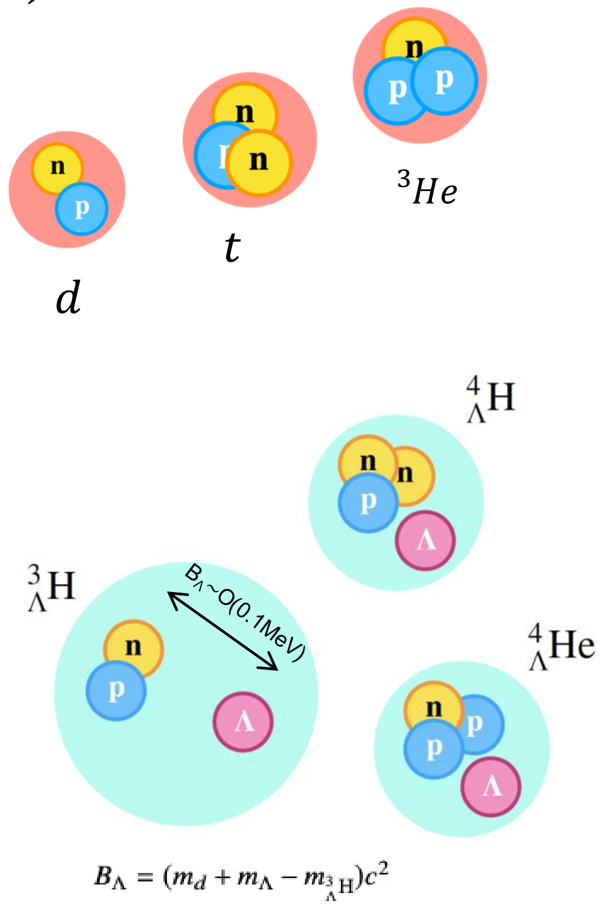

Hypernuclei (Why)

1. What can (hyper)nuclei production in heavy-ion collisions tell us about the QCD phase diagram and the nuclear equation-of-state?

- Sensitive to critical fluctuations and the onset of deconfinement

$$\frac{t \times p}{d^2}$$

Sensitive to neutron density fluctuations

$$\frac{{}^3_\Lambda\mathrm{H}}{{}^3\mathrm{He} \times \frac{\Lambda}{\mathrm{p}}}$$

Sensitive to baryon-strangeness correlations

2. What is the role of hyperon-nucleon (Y-N) and hyperon-hyperon (Y-Y) interaction (or even Y-N-N) in the equation-of-state of high baryon density matter

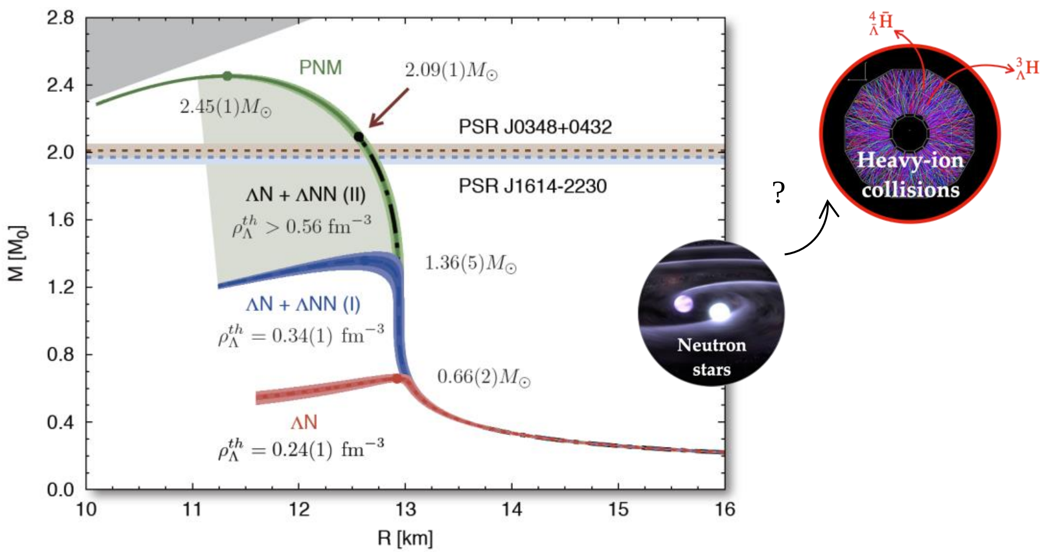

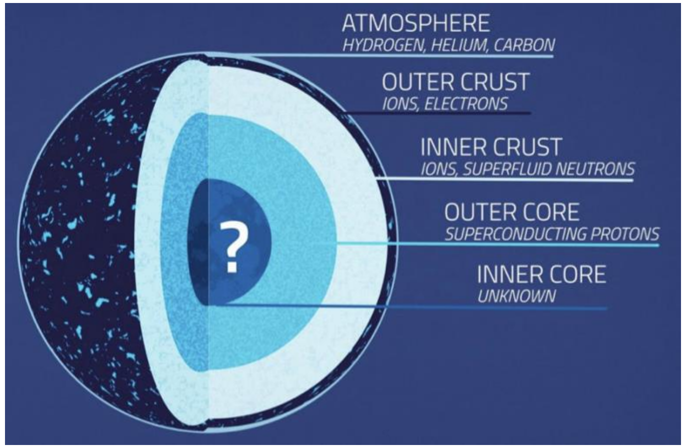

EoS governs the structure of neutron stars.

- Hyperon Puzzle: difficulty to reconcile the measured masses of neutron stars with the presence of hyperons in their interiors

Hypernuclei (How)

1. Intrinsic properties: Internal structure
   - Lifetime, branching ratio, binding energy, etc.

Understanding hypernuclei structure can provide insights to the Y-N interaction and EoS (especially in high baryon density region, to study the density dependence)

Fig. from Yifei

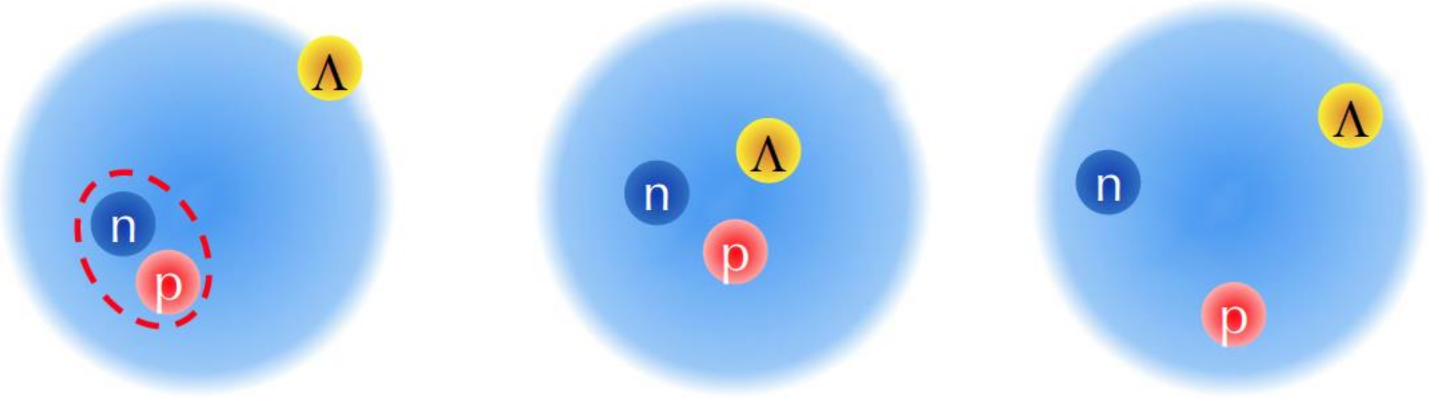

Hypernuclei (How)

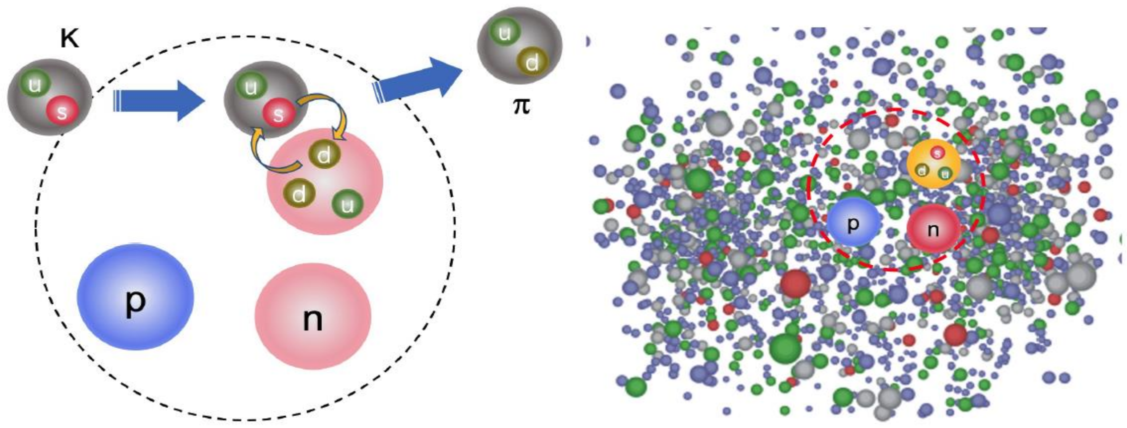

Fig. from Yifei

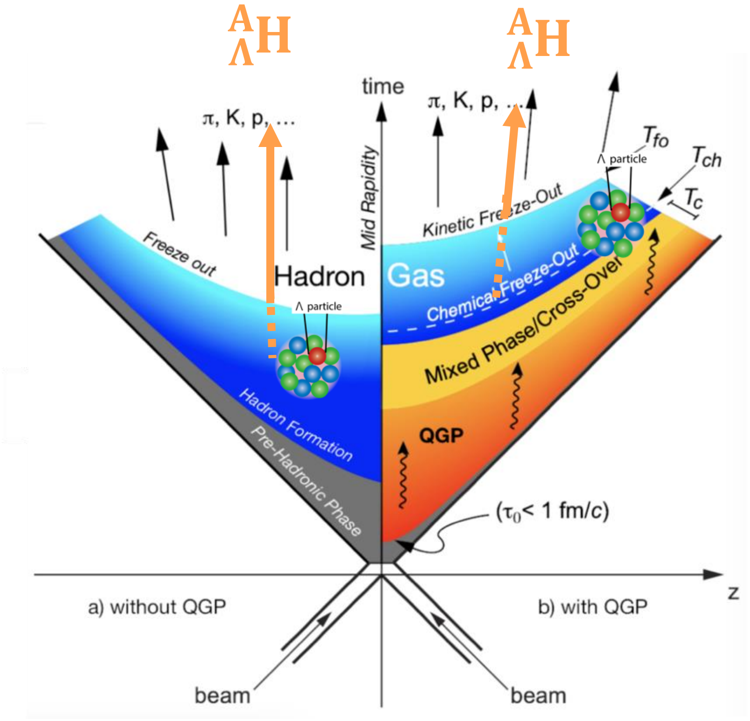

When are hypernuclei formed?
At freezeout? Or in medium?

2. Production mechanism (in heavy-ion collisions)

- Spectra, Yields, Collectivity etc

The process of hypernuclei formation in violent heavy-ion collisions is not well understood

Y-N Interactions from Non-HICs

Important, but lack of measurements limited by availability and short-lifetime of hyperon beams

Some new interesting results on hyperon-nucleon scattering at BESIII, the idea is simple, using J/ψ decayed hyperons, to interact with the beam pipe (Be)

CLAS/J-PARC
BESIII

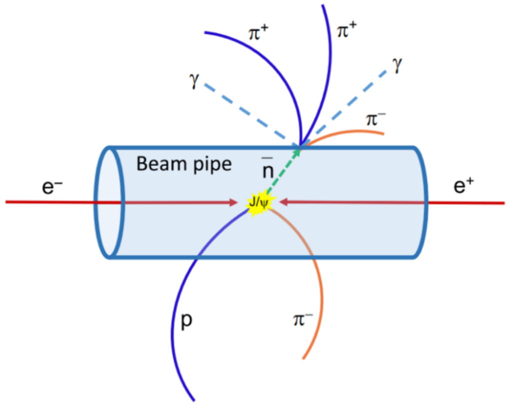

Phys. Rev. Lett. 127, 012003 (2021)
arXiv: 2209.12601 Chin.Phys.C 48 (2024)

$\bar{n}p \rightarrow \pi^+\pi^+\pi^-\pi^0, \pi^0 \rightarrow \gamma\gamma$

10 billion J/ψ

$\Xi^0 n \rightarrow \Xi^- p$ $\Lambda N \rightarrow \Sigma^+ X$

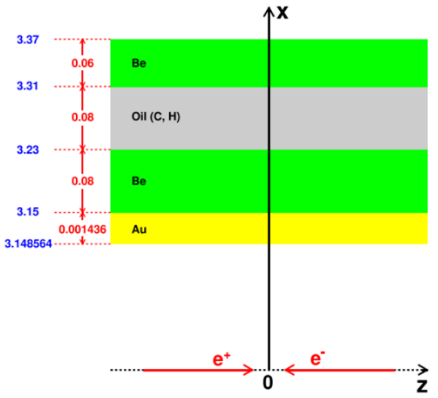

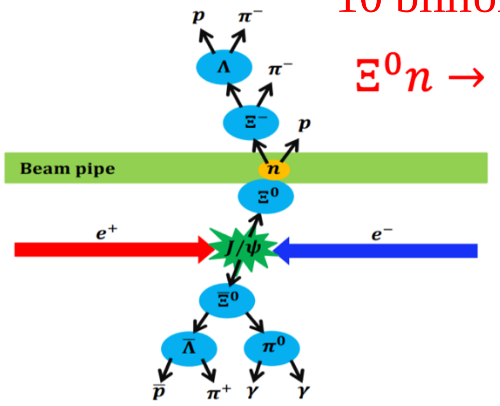

particle source: hyperon from J/ψ decays
target material: beam pipe
detector: BESIII detector

From Jielei @ Huizhou Hyperon workshop

Phys. Rev. Lett. 130, 251902 (2023)
Phys. Rev. C 109, L052201 (2024)
Phys. Rev. Lett. 132 (2024) 23, 231902

$\Lambda p \rightarrow \Lambda p$ and $\bar{\Lambda}p \rightarrow \bar{\Lambda}p$

Hyperon/Antihyperon	τ ($\times 10^{-10}$s)	Decay mode	$\mathcal{B}$ ($\times 10^{-3}$)	P (GeV/c)
$\Lambda/\bar{\Lambda}$	2.63	$J/\psi \rightarrow \Lambda\bar{\Lambda}$	1.89	1.074
$\Sigma^+/\bar{\Sigma}^-$	0.80	$J/\psi \rightarrow \Sigma^+\bar{\Sigma}^-$	1.07	0.992
$\Xi^0/\bar{\Xi}^0$	2.90	$J/\psi \rightarrow \Xi^0\bar{\Xi}^0$	1.17	0.818
$\Xi^-/\bar{\Xi}^+$	1.64	$J/\psi \rightarrow \Xi^-\bar{\Xi}^+$	0.97	0.807
$\Lambda/\bar{\Lambda}$	2.63	$\psi(2S) \rightarrow \Lambda\bar{\Lambda}$	0.38	1.467
$\Sigma^+/\bar{\Sigma}^-$	0.80	$\psi(2S) \rightarrow \Sigma^+\bar{\Sigma}^-$	0.24	1.408
$\Xi^0/\bar{\Xi}^0$	2.90	$\psi(2S) \rightarrow \Xi^0\bar{\Xi}^0$	0.23	1.291
$\Xi^-/\bar{\Xi}^+$	1.64	$\psi(2S) \rightarrow \Xi^-\bar{\Xi}^+$	0.29	1.284
$\Omega^-/\bar{\Omega}^+$	0.82	$\psi(2S) \rightarrow \Omega^-\bar{\Omega}^+$	0.06	0.774

Why Hypernuclei in HIC ? (at High Baryon Density)

Why heavy-ion collisions (HIC)?

- produced in copious amounts in HIC
- Potential for high precision measurements
- Big advantages at high μ_B: enhanced yields

- Collider mode： $\sqrt{s_{NN}}$ = 7.7 - 54GeV
- Fixed-Target mode： $\sqrt{s_{NN}}$ = 3.0 - 13.7GeV

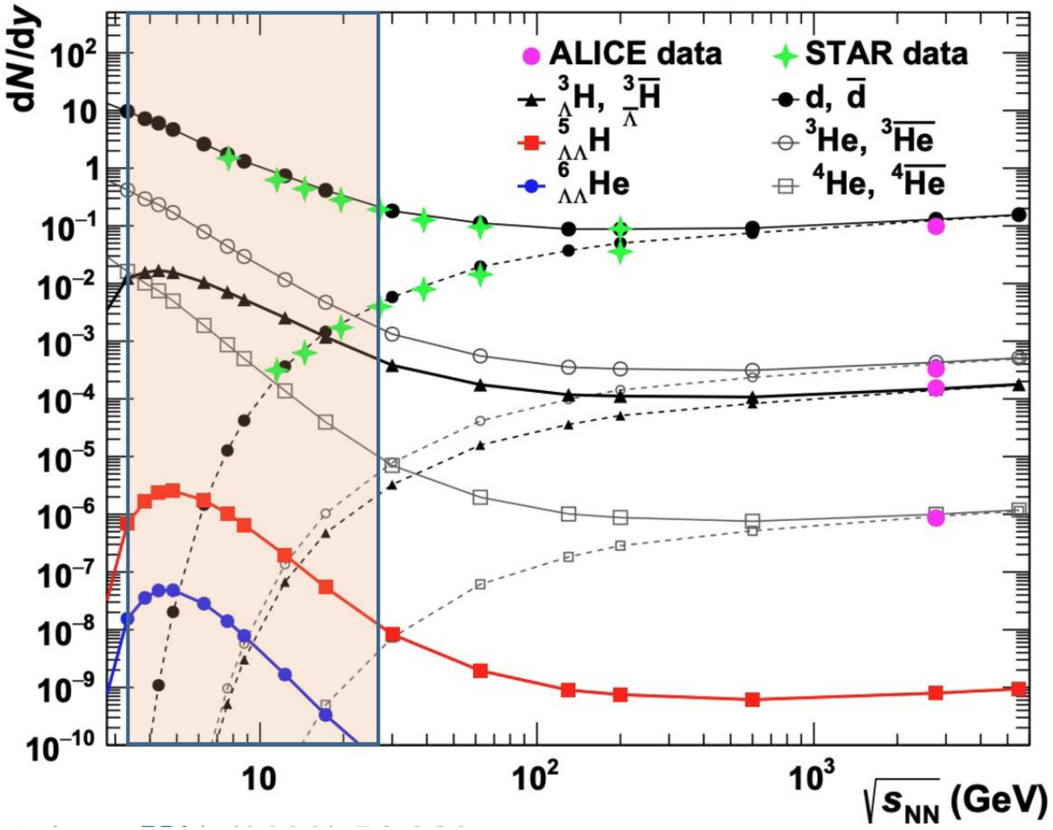

B. Dönigus, EPJA (2020) 56:280

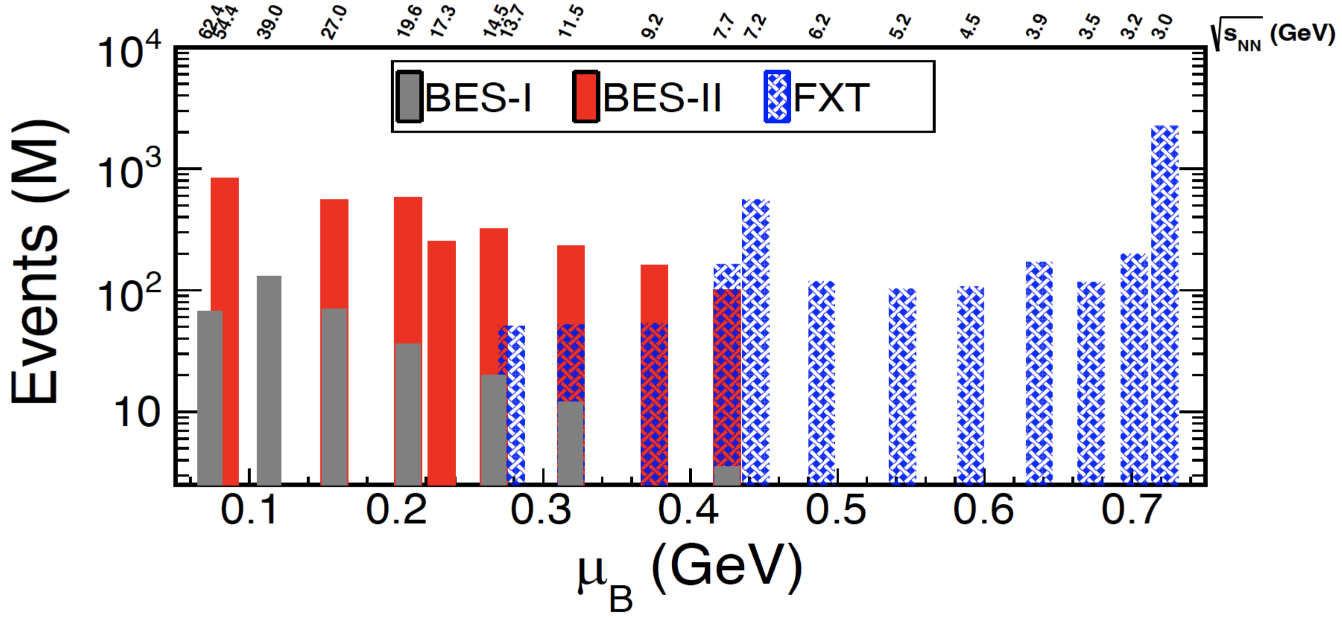

$3 < \sqrt{s_{NN}} < 200\ GeV; 760 > \mu_B > 25\ MeV;$

STAR Experimental

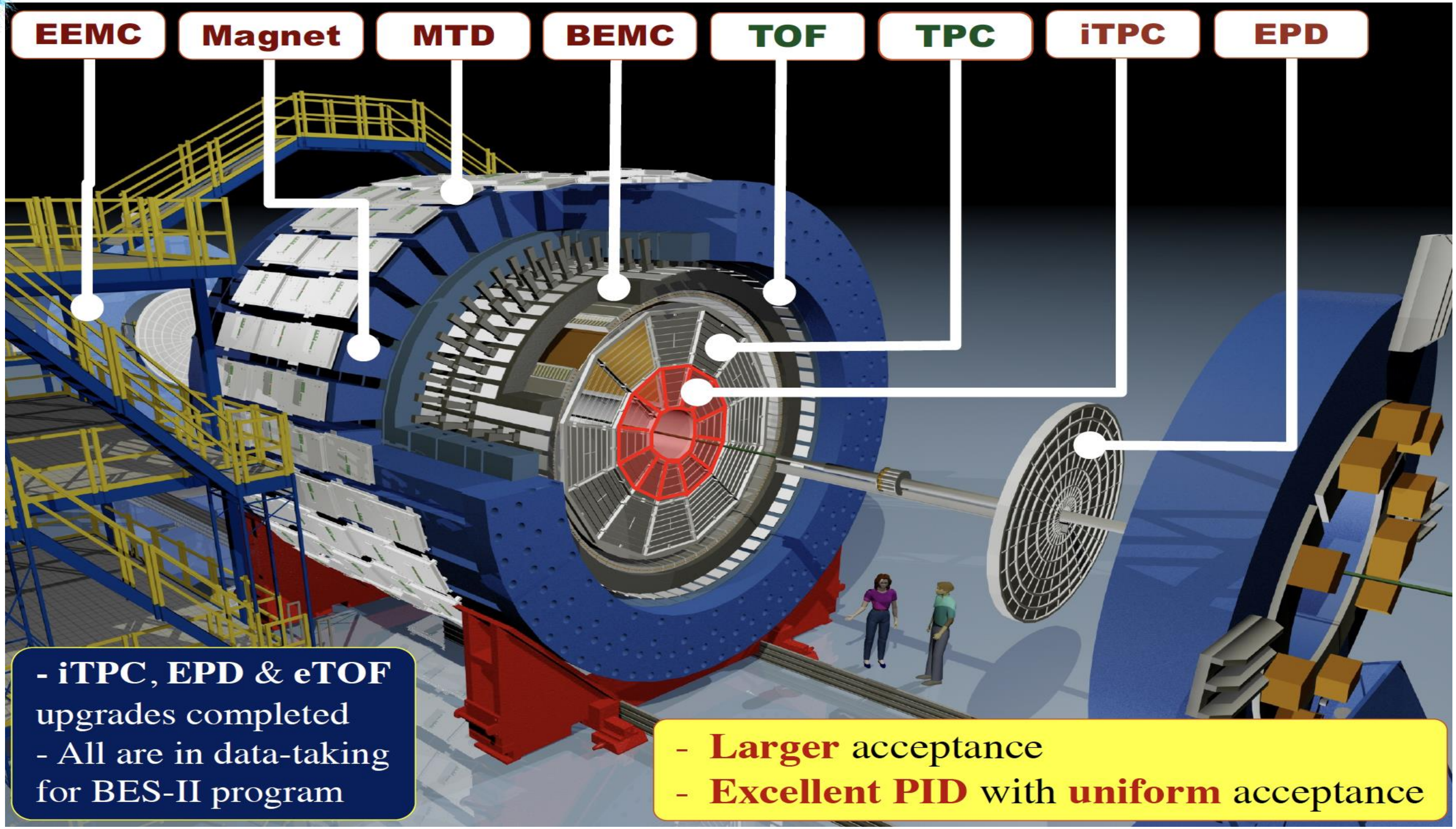

FXT Setup @ STAR

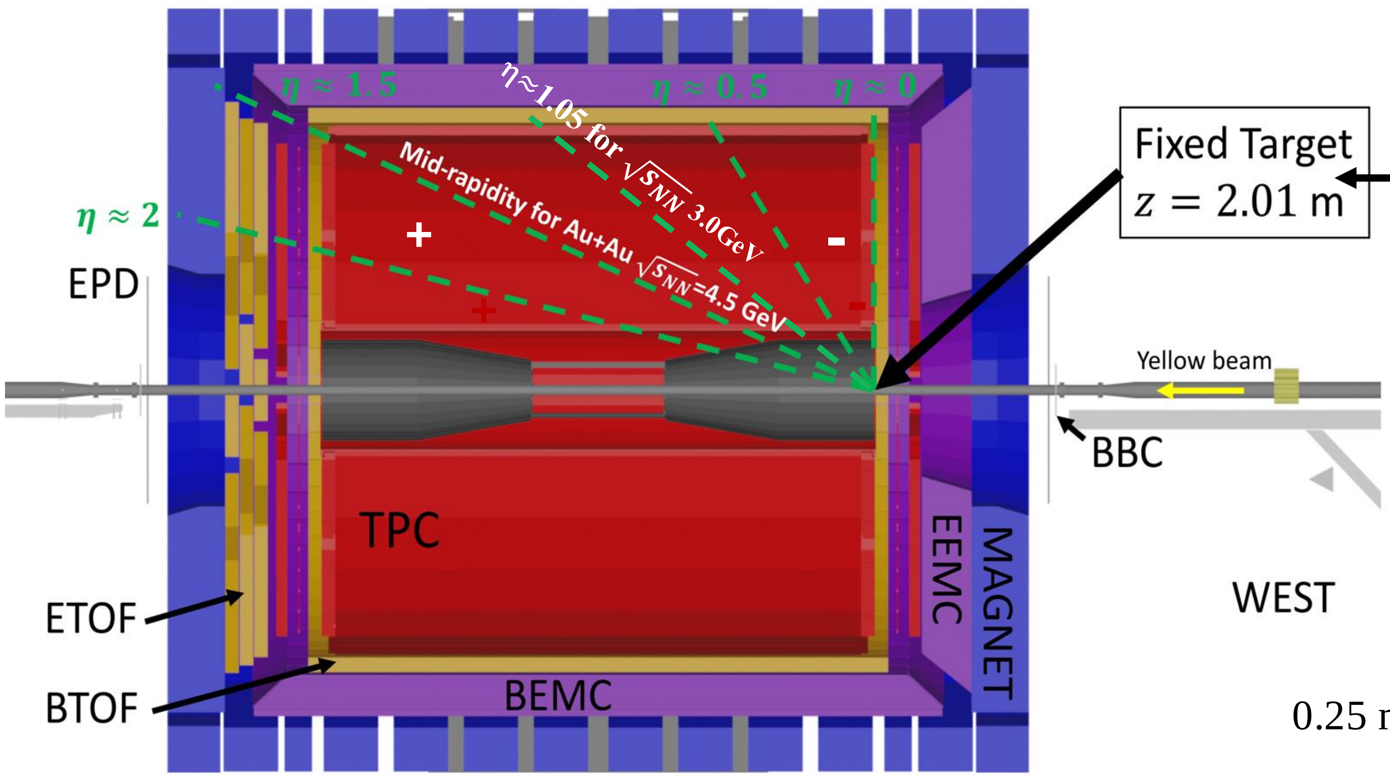

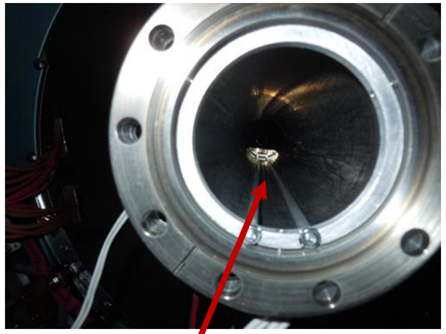

0.25 mm thickness Au-Target

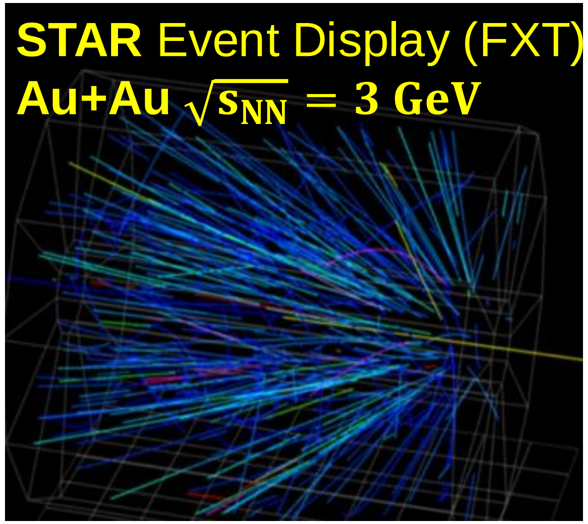

Good mid-rapidity coverage for STAR FXT 3 GeV (and up to 4.5GeV)

Conventions: beam-going direction is the positive direction

Hypernuclei Reconstruction

Phys. Rev. Lett. 128 (2022) 20, 202301

Two body decay: ${}^{3}_{\Lambda}H \rightarrow {}^{3}He\,\pi^{-}$; ${}^{4}_{\Lambda}H \rightarrow {}^{4}He\,\pi^{-}$

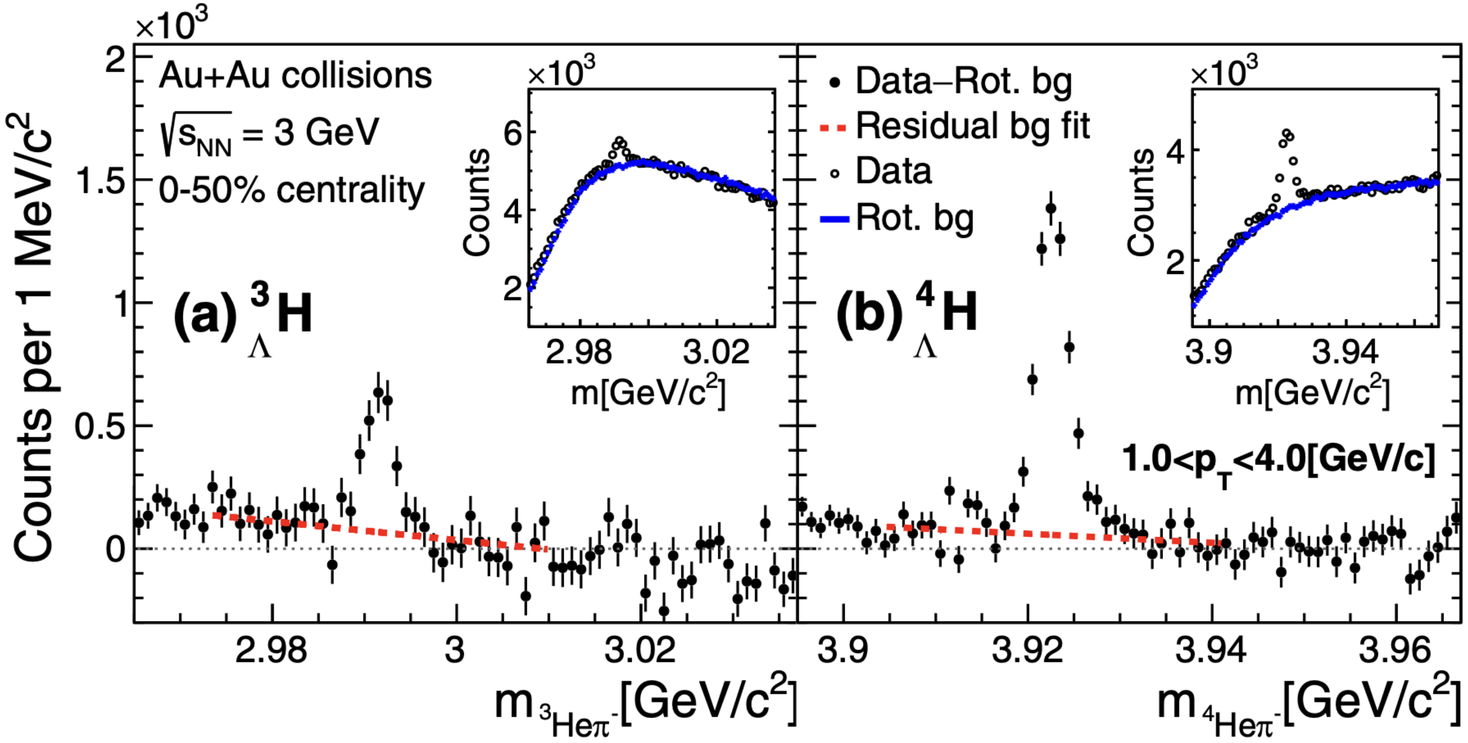

Hypertriton results from
3.0 3.2, 3.5, 3.9, 4.5, 5.2 GeV (FXT)
7.7, 11.5, 14.6 GeV (COL)

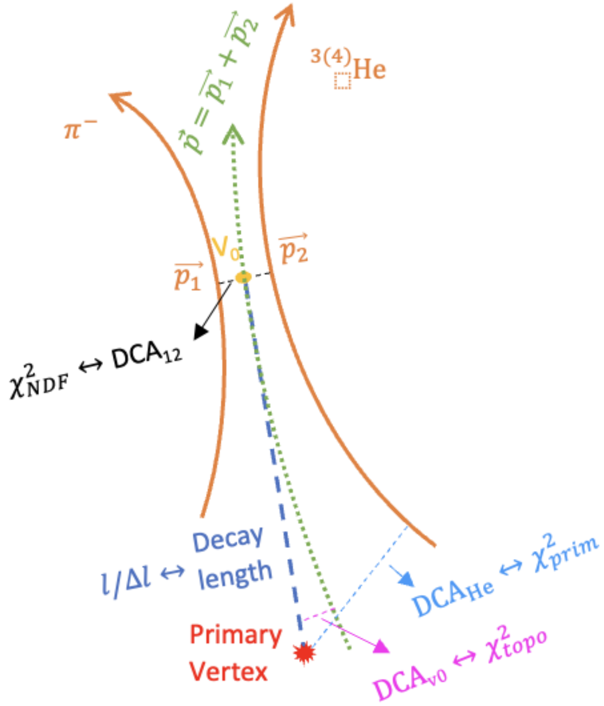

Hypernuclei Reconstruction

Y. Ji. C. Hu, X. Li, STAR, sQM 2024

Three body decay: ${}^{3}_{\Lambda}H \rightarrow \mathrm{p\,d}\,\pi^{+}$; ${}^{4}_{\Lambda}He \rightarrow {}^{3}He\,\mathrm{p}\,\pi^{+}$

New results from 3.0, 3.2, 3.5 GeV (FXT)

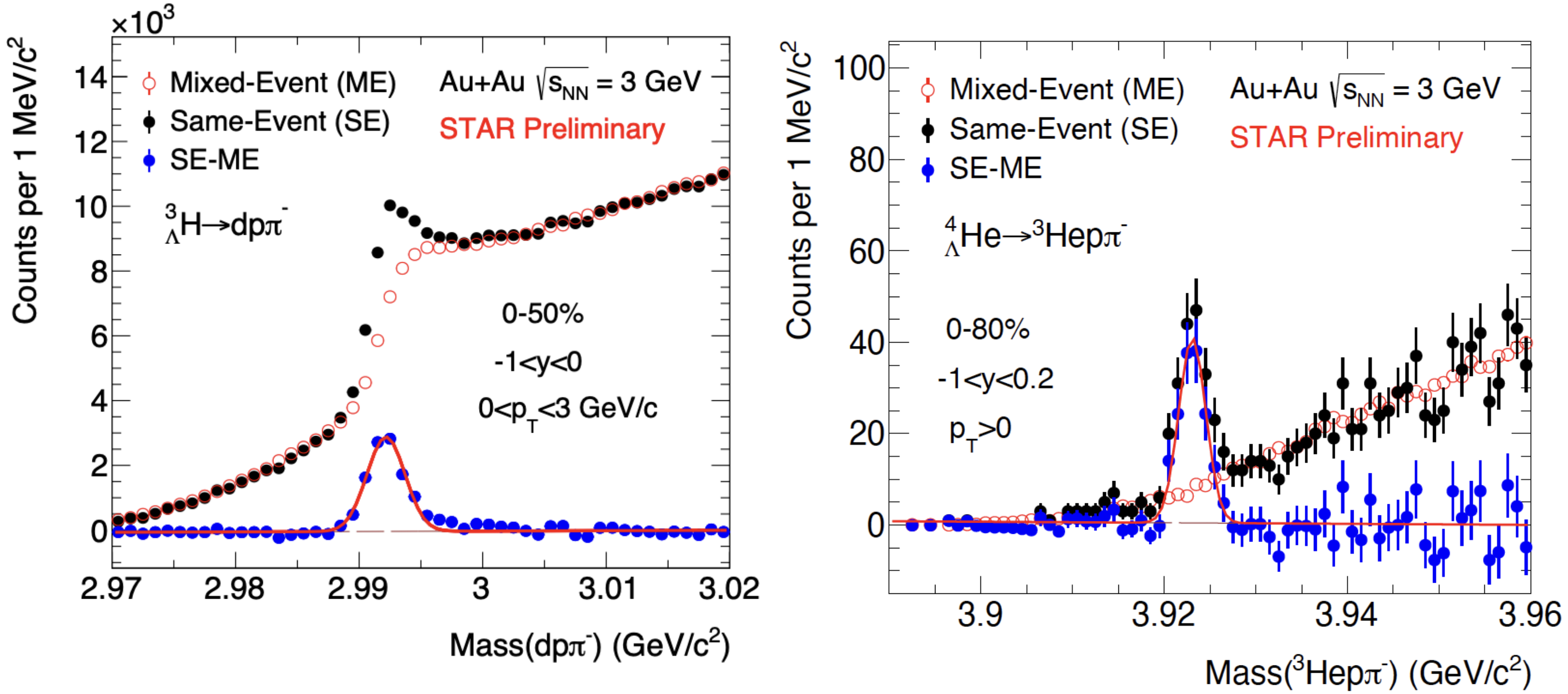

- Measurement of Hypernuclei Intrinsic Properties:

  -- Lifetime, Branch Ratios & Binding Energy

Hypernuclei Lifetime

Phys. Rev. Lett. 128 (2022) 20, 202301

- Light hypernuclei inner structure serves for our understanding of the YN interaction

Lifetime

$$N(\tau) = N_0 e^{-L/\beta\gamma c\tau}$$

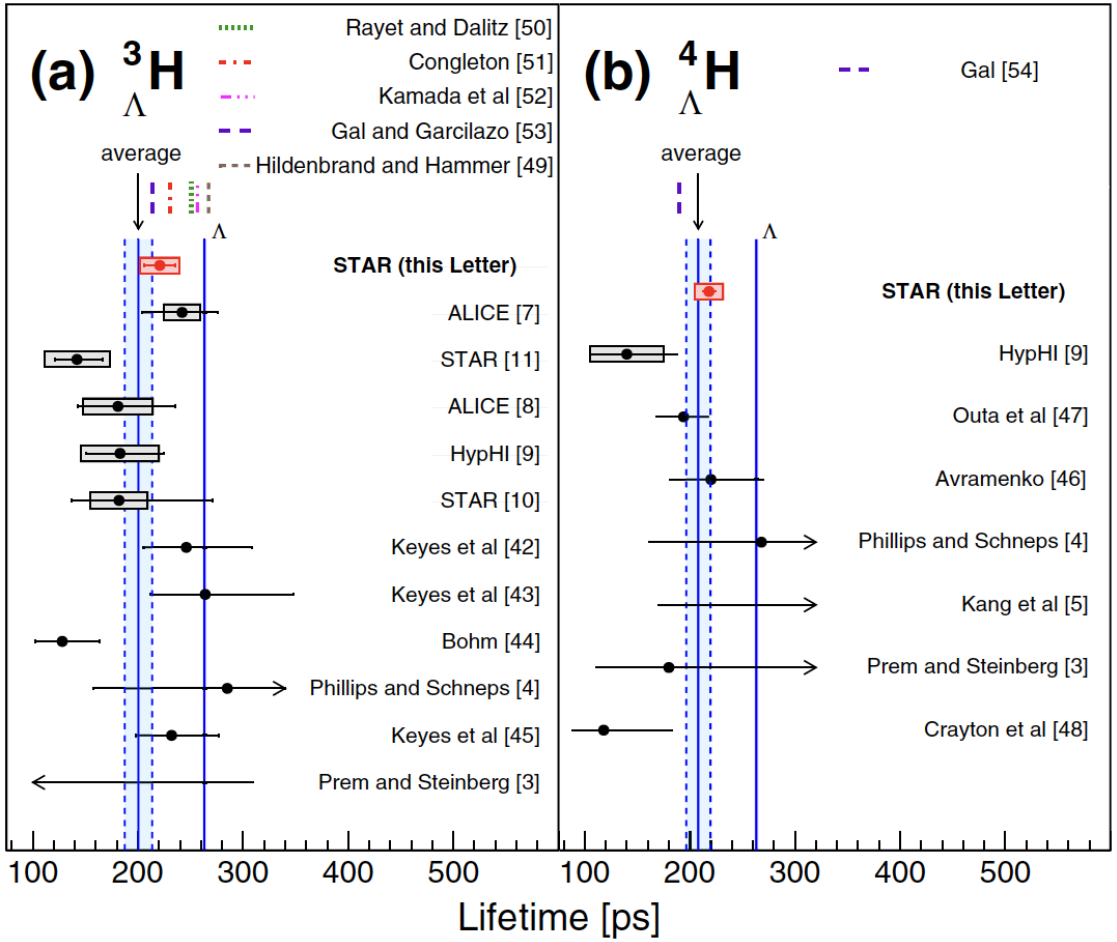

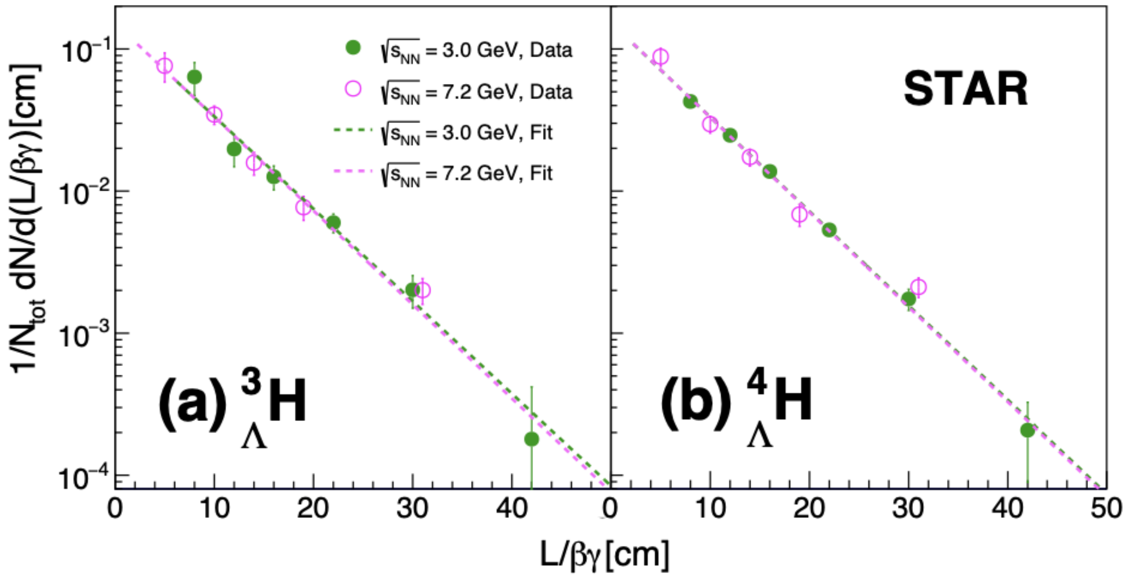

$^{3}_{\Lambda}$H: Global avg. = (87±5)%$\tau(\Lambda)$, 2.8σ< $\tau(\Lambda)$.

- Calculations with pion FSI consistent with data.

A. Gal, EPJ Web Conf. 259, 08002 (2022) A. Gal et al, PLB791, 48 (2019)

Hypernuclei Lifetime

- Light hypernuclei inner structure serves for our understanding of the YN interaction

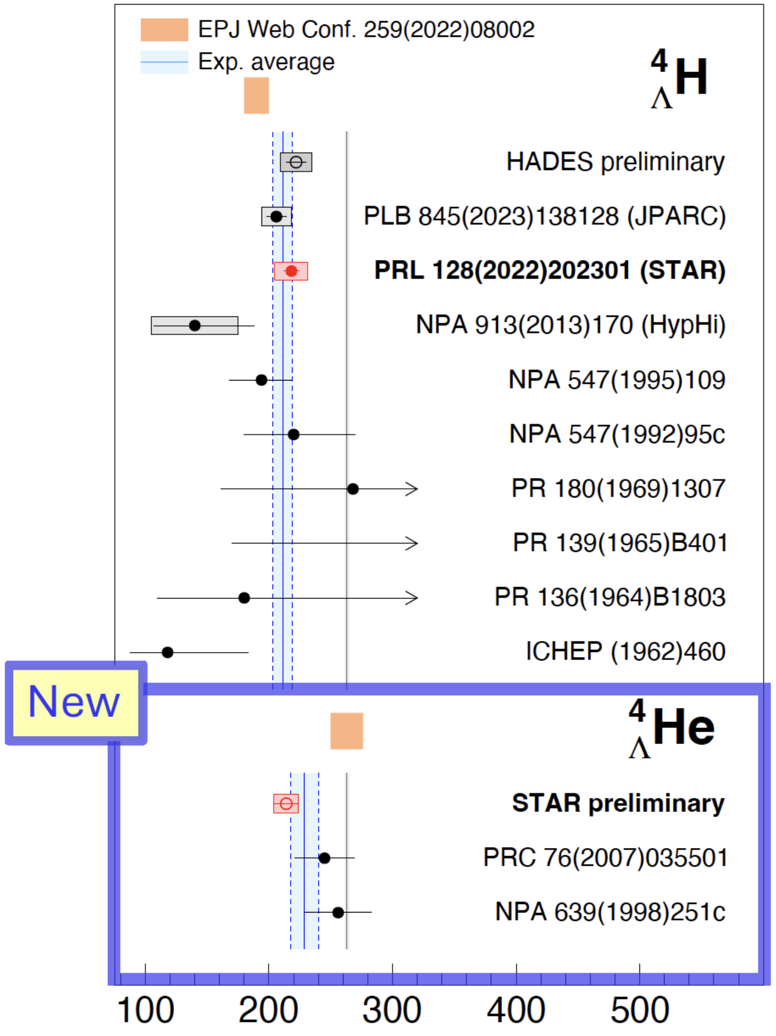

Lifetime

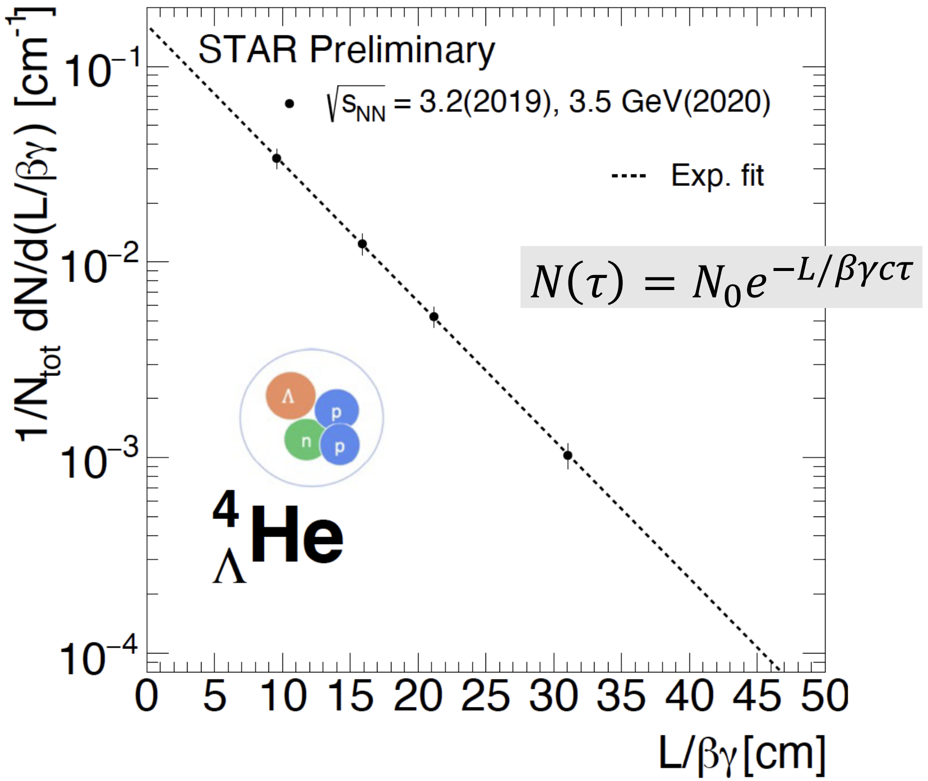

- Lifetime ratio based on isospin rule. $\frac{\Gamma({}^{4}_{\Lambda}\mathrm{He} \to {}^{4}\mathrm{He} + \pi^0)}{\Gamma({}^{4}_{\Lambda}\mathrm{H} \to {}^{4}\mathrm{He} + \pi^-)} \approx \frac{1}{2}$
- New data ${}^{4}_{\Lambda}\mathrm{He}$: $214 \pm 10 \pm 10\ ps$, most precise to date
- Shorter than $\tau(\Lambda)$ by 3σ; $\tau({}^{4}_{\Lambda}\mathrm{H})/\tau({}^{4}_{\Lambda}\mathrm{He}) = 0.92 \pm 0.06$.

A. Gal, EPJ Web Conf. 259, 08002 (2022) A. Gal et al, PLB791, 48 (2019)

Hypertriton Branching Ratio

- Stronger constraints on absolute B.R. and hypertriton internal structure models
- Model comparison show data favors small B_Λ, weakly bounded state of ${}^3_\Lambda H$

$$R_3 = \frac{B.R.({}^3_\Lambda H \rightarrow {}^3He\,\pi^-)}{B.R.({}^3_\Lambda H \rightarrow p\,d\,\pi^-) + B.R.({}^3_\Lambda H \rightarrow {}^3He\,\pi^-)}$$

STAR: $R_3 = 0.272 \pm 0.030 \pm 0.042$

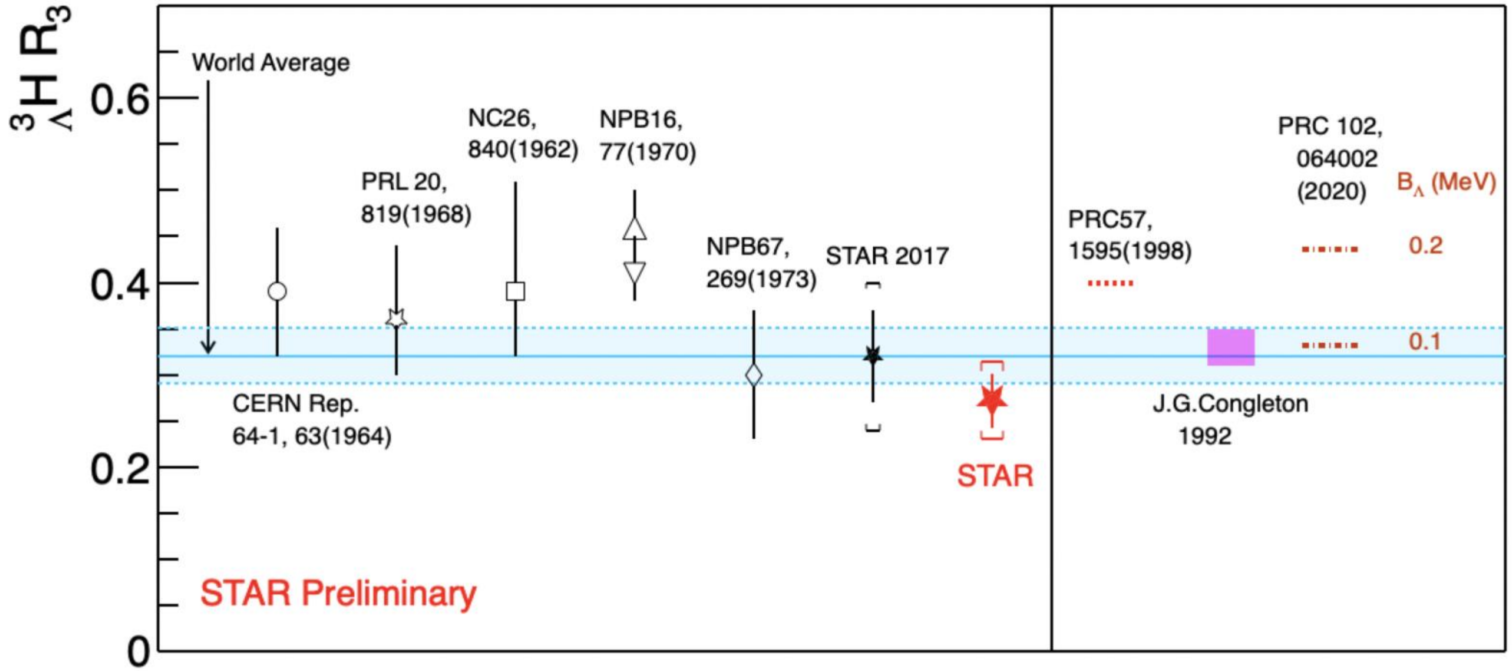

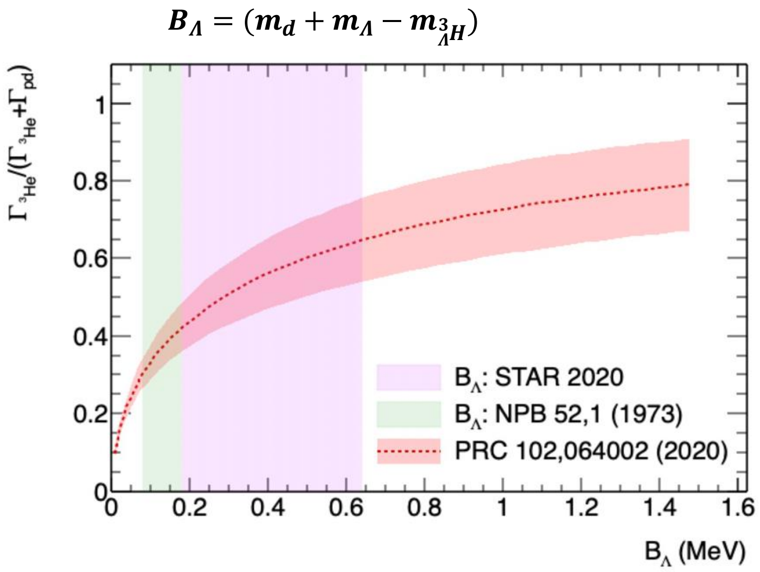

${}^{3}_{\Lambda}$H Separation Energy (B_Λ)

- Λ separation energy (B_Λ): ${}^{3}_{\Lambda}\mathrm{H}\ B_\Lambda = \mathrm{M}(d) + \mathrm{M}(\Lambda) - \mathrm{M}({}^{3}_{\Lambda}\mathrm{H})$
  - Benchmark of Y-N interaction strength

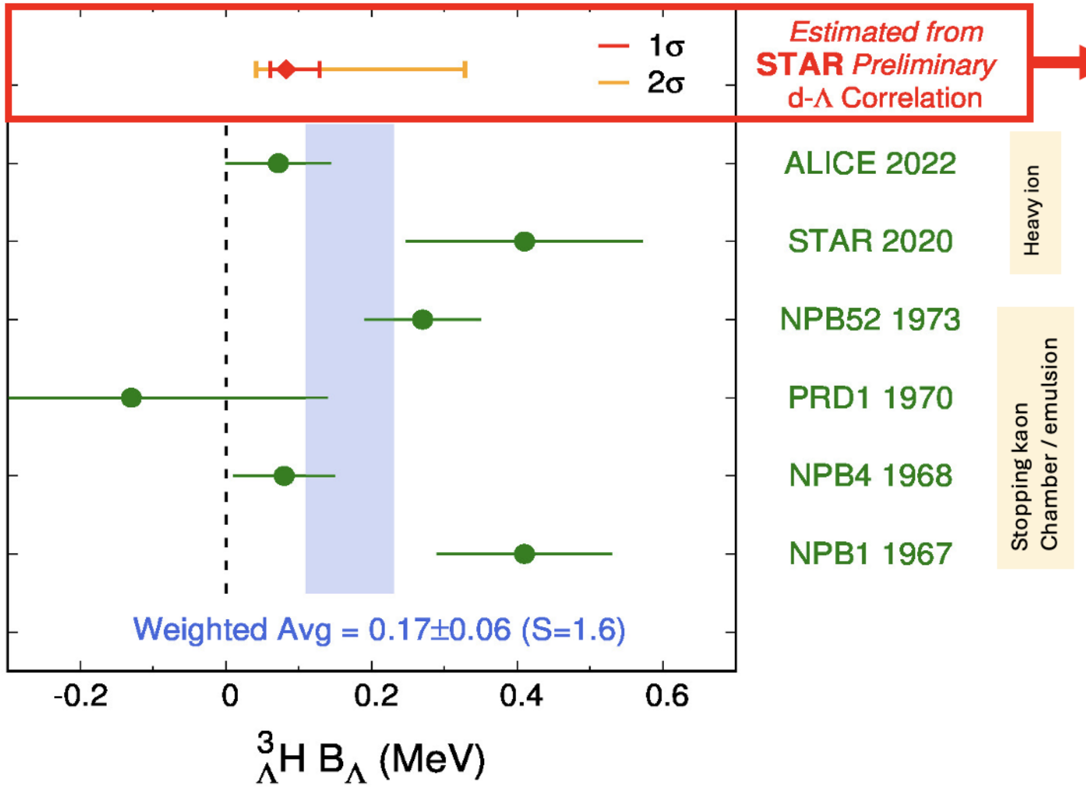

- Invariant mass method
- Femtoscopy method
  - $\frac{1}{-f_0} = \gamma - \frac{1}{2} d_0 \gamma^2,\ B_\Lambda = \frac{\gamma^2}{2\mu_{d\Lambda}}$

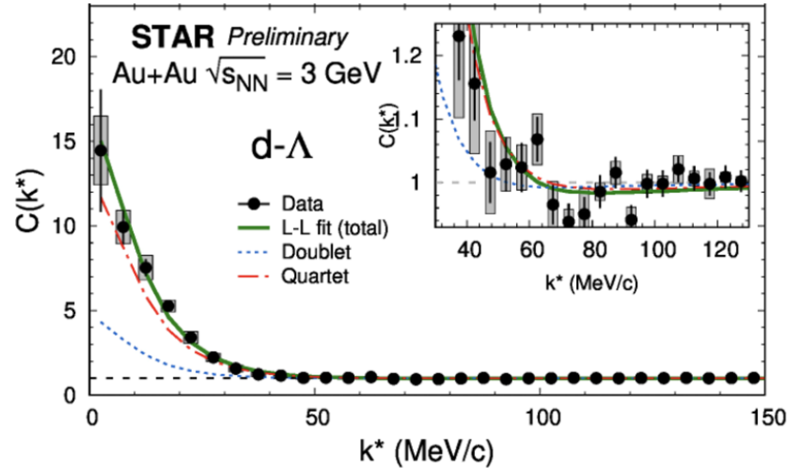

- ${}^{3}_{\Lambda}$H is a very loosely bound state.

- Measurement of Hypernuclei Production

  -- Energy Dependence of Hypernuclei Production

A=3 Hypernuclei from BES-II Energies

Phys. Rev. Lett. 128 (2022) 20, 202301 @ 3 GeV
New ${}^{3}_{\Lambda}$H *results @ 3.2, 3.5, 3.9, 4.5, 5.2 (FXT)*
@ 7.7, 11.5 14.6GeV (Coll.) from sQM2024

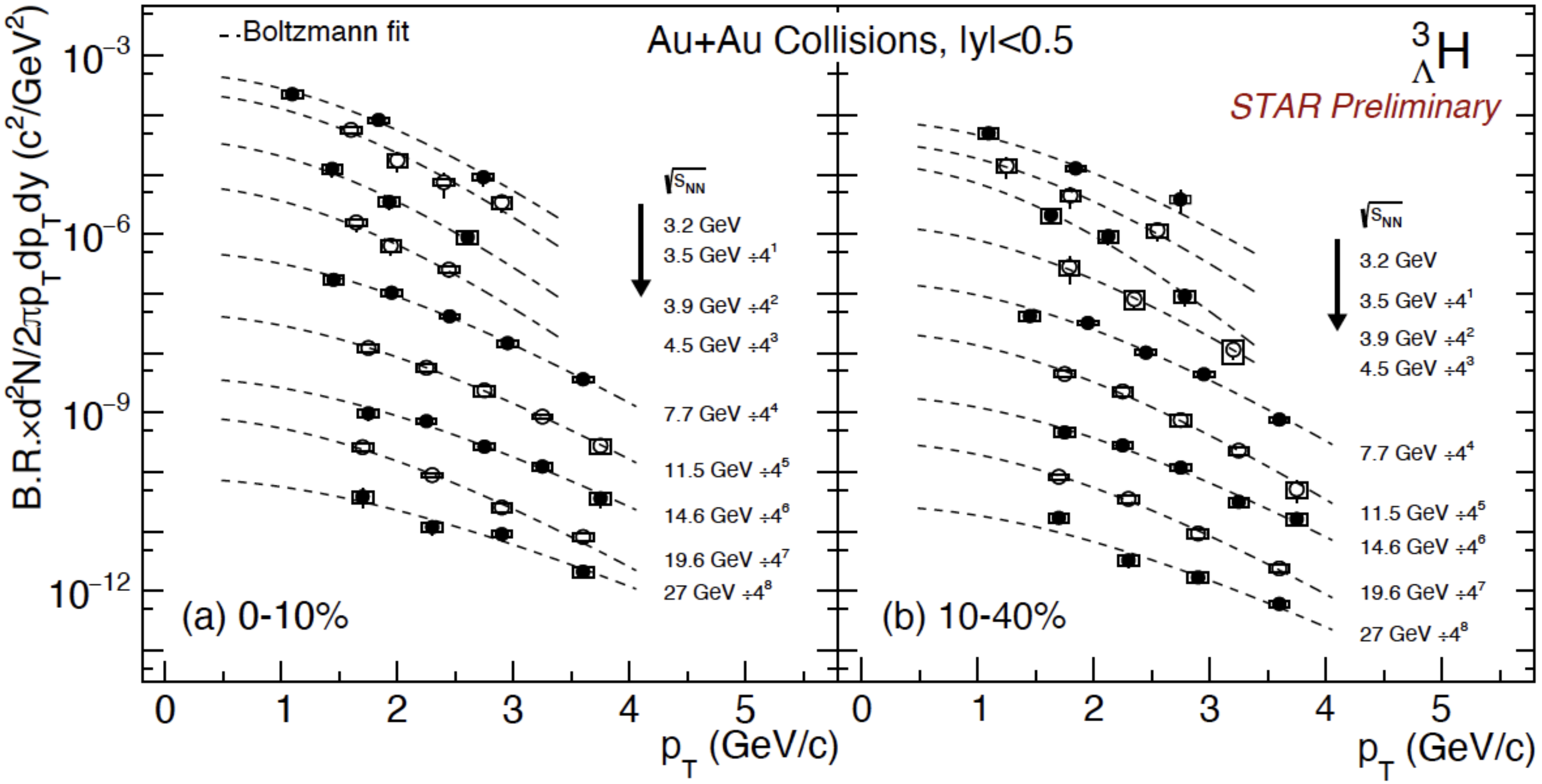

Utilizing datasets collected by STAR BES,
- ${}^{3}_{\Lambda}$H p_T spectra, dN/dy are measured at $\sqrt{(s_{NN})}$= 3-27 GeV in Au+Au collisions.

A=3 Hypernuclei Yields vs. Rapidity

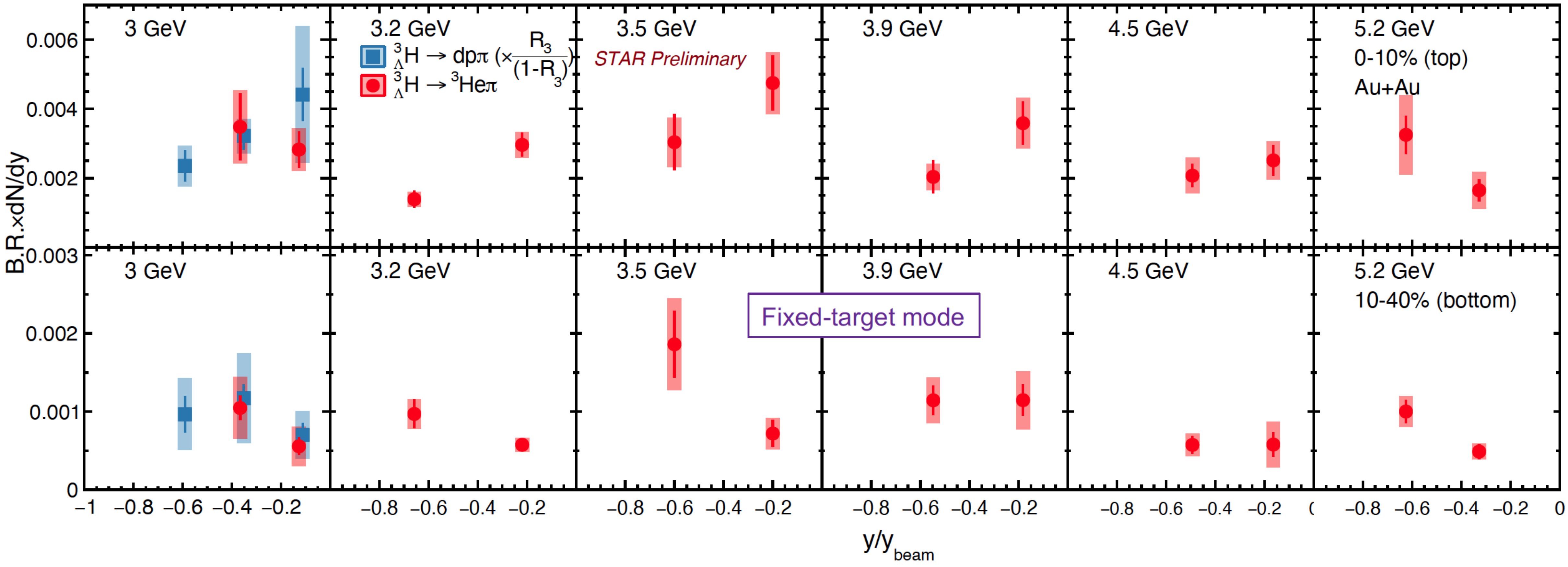

First measurements on rapidity dependence of hypernuclei yields in HIC, consist b/w 2 body and 3 body.
Different trends in rapidity in 10-40% centrality regions. -> Fragmentation contribution

A=4 Hypernuclei from BES-II Energies

New ${}^{4}_{\Lambda}$H(e) results @ 3.0, 3.2, 3.5, (FXT) from sQM2024

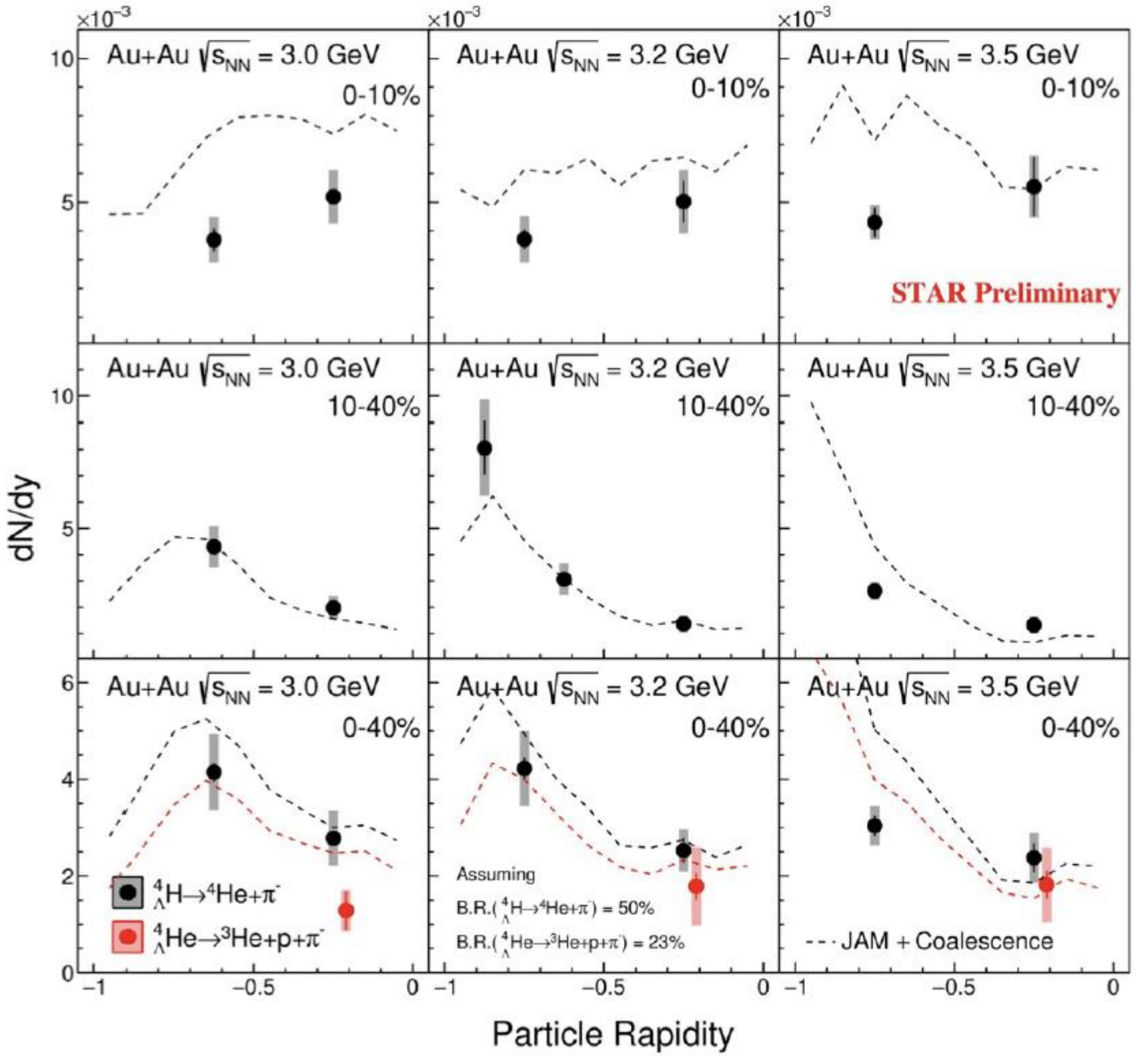

- ${}^{4}_{\Lambda}$H(e) p_T spectra, dN/dy are measured at $\sqrt{(s_{NN})}$= 3-3.5 GeV in Au+Au collisions.

Hypernuclei Yield vs. $\sqrt{s_{NN}}$

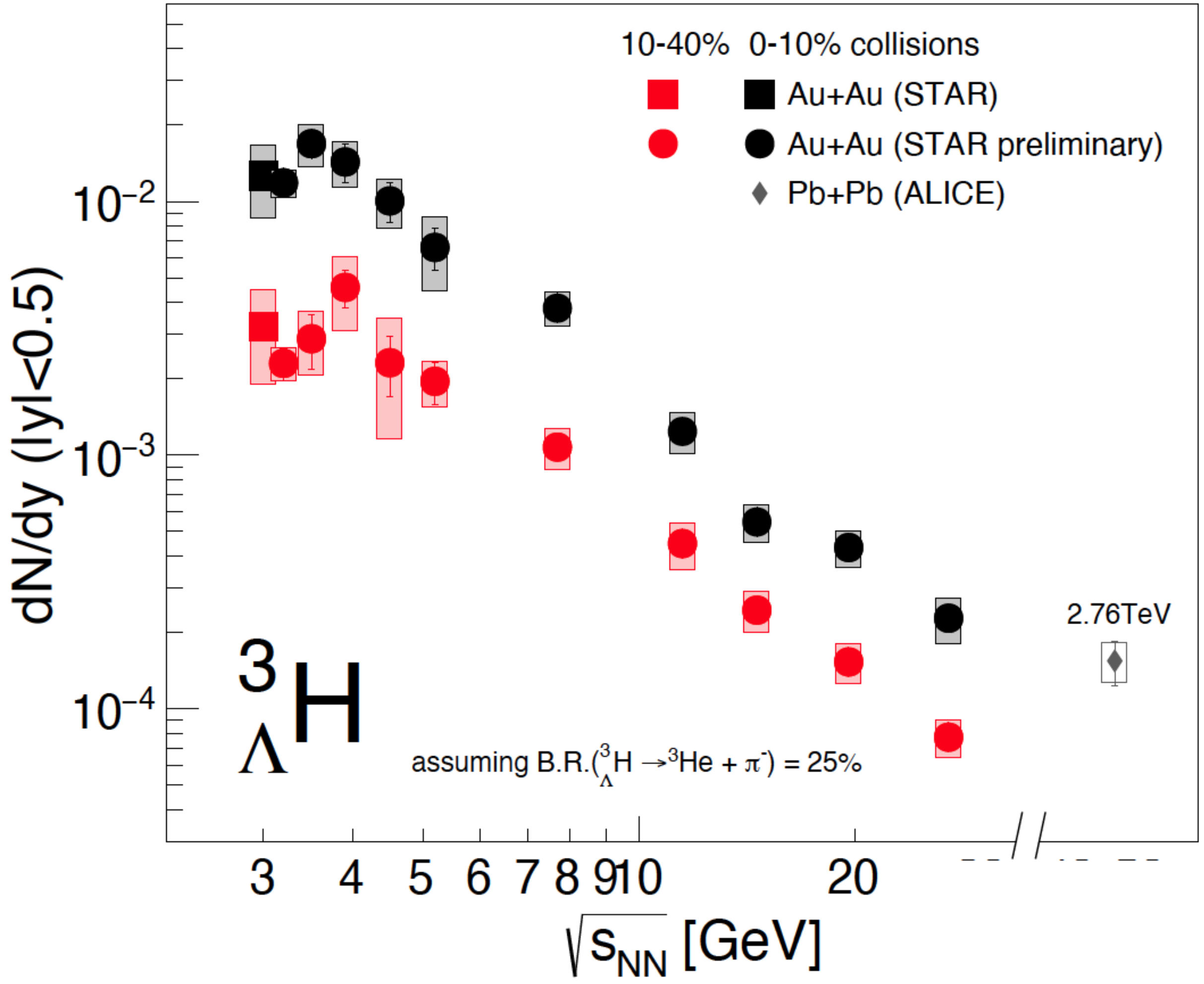

First energy dependence of $^{3}_{\Lambda}H$ hypernuclei production yields in high baryon region

$^{3}_{\Lambda}H$ yields peak at $\sqrt{(s_{NN})}$ = 3-4 GeV then decrease toward higher energy

- Increasing baryon density at lower energies ↑
- Stronger strangeness canonical suppression at low energies ↓

Low Energies 3-4GeV optimal range search for $\Lambda\Lambda$-hypernuclei

Pb+Pb: ALICE, PLB 754, 360 (2016)
STAR at 3 GeV: PRL 128, 202301 (2022)

Hypernuclei Yield vs. $\sqrt{s_{NN}}$

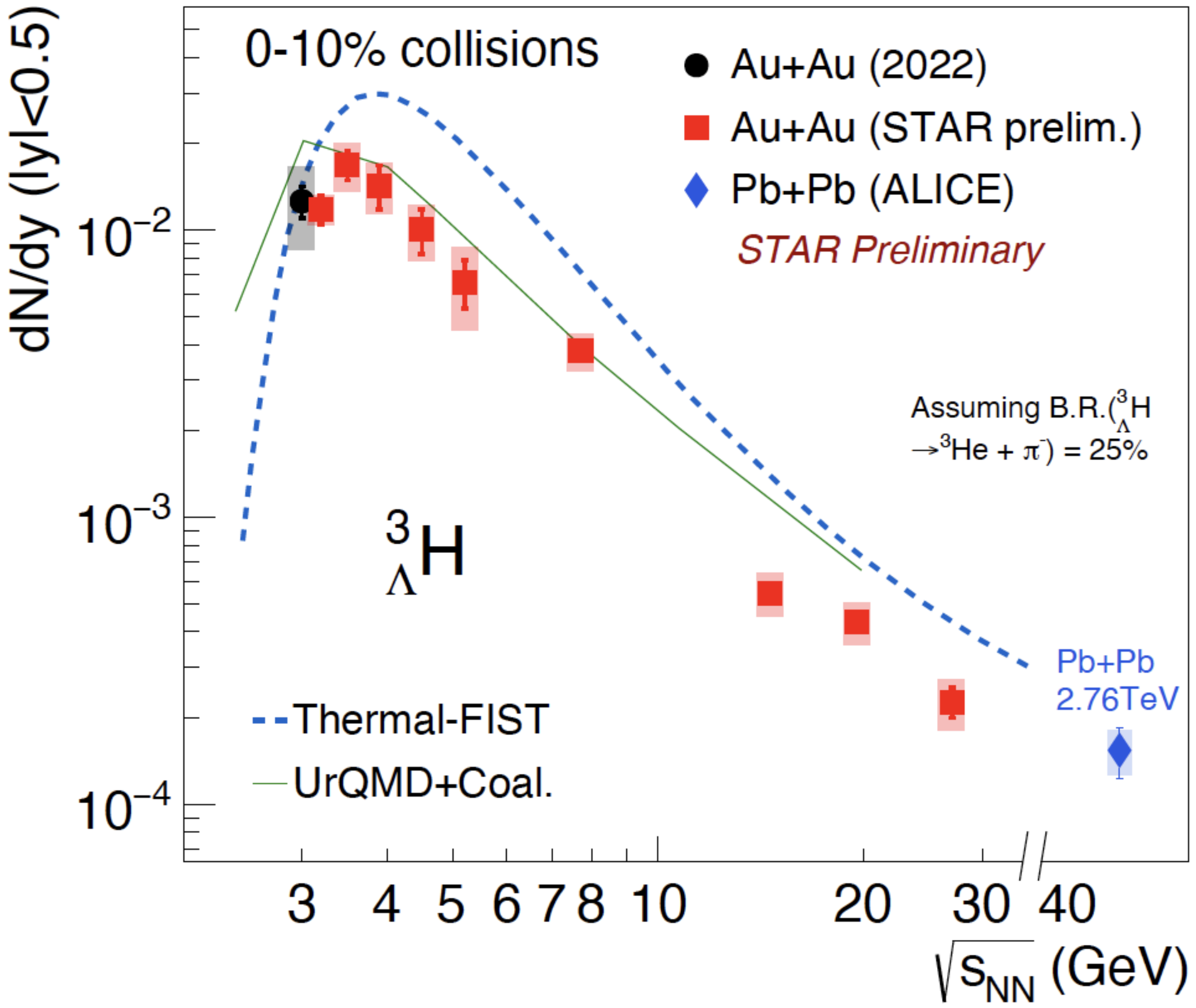

Thermal model
Hadron chemical freeze-out T_{ch} and μ_B.

UrQMD + Coal.
Instant coalescence after hadron kinetic freeze-out.
Coalescence condition:
- $|\vec{p_1} - \vec{p_2}| < \Delta P, \ |\vec{r_1} - \vec{r_2}| < \Delta R$

or Wigner Coalescence

Provide first constraints for hypernuclei production models in the high-baryon-density region

Thermal (GSI): A. Andronic et al. PLB 697,203-207 (2011)
Thermal-FIST, Coal. (UrQMD): T. Reichert et al. PRC 107 (2023) 1, 014912

Hypernuclei Yield vs. $\sqrt{s_{NN}}$

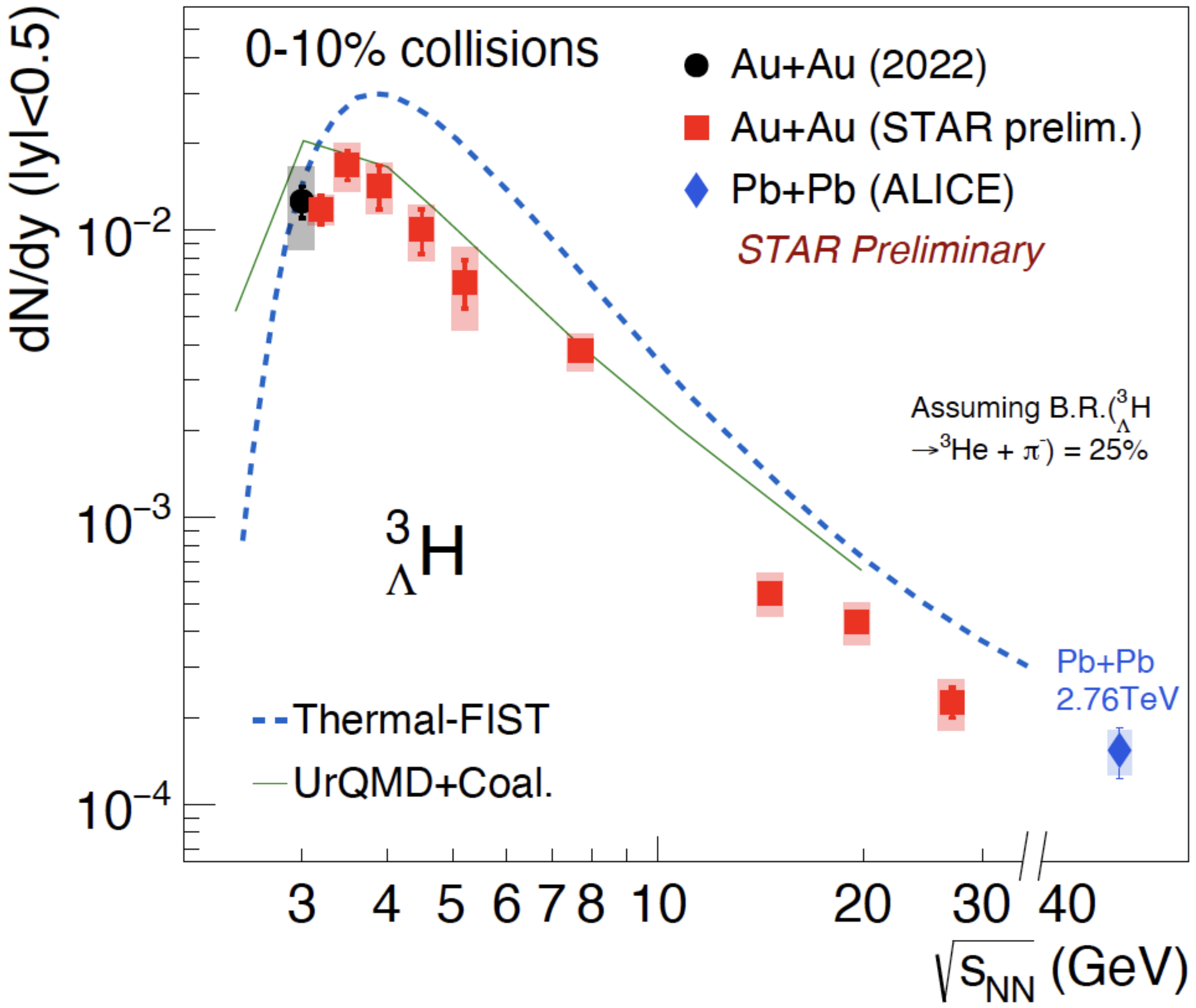

Thermal model
Hadron chemical freeze-out T_{ch} and μ_B.

Both hypertriton and triton yields are not fixed at chemical freeze-out (disfavor thermal)

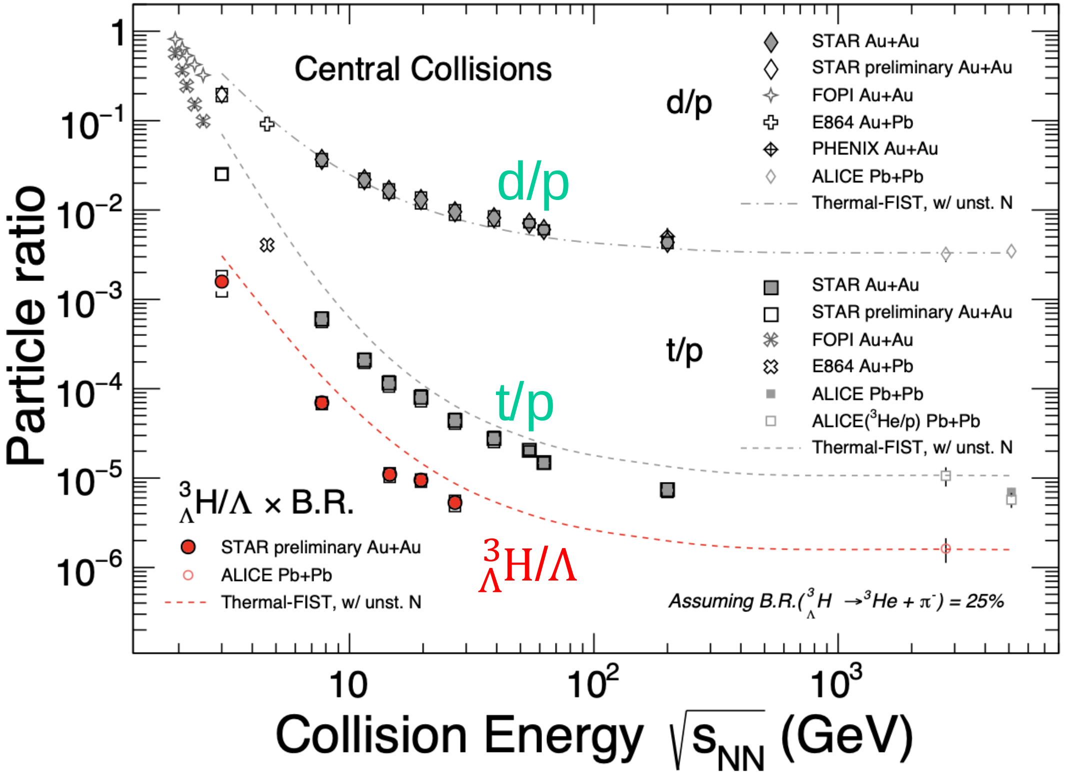

Thermal (GSI): A. Andronic et al. PLB 697,203-207 (2011)
Thermal-FIST, Coal. (UrQMD): T. Reichert et al. PRC 107 (2023) 1, 014912

A=4 Hypernuclei Yield Ratios

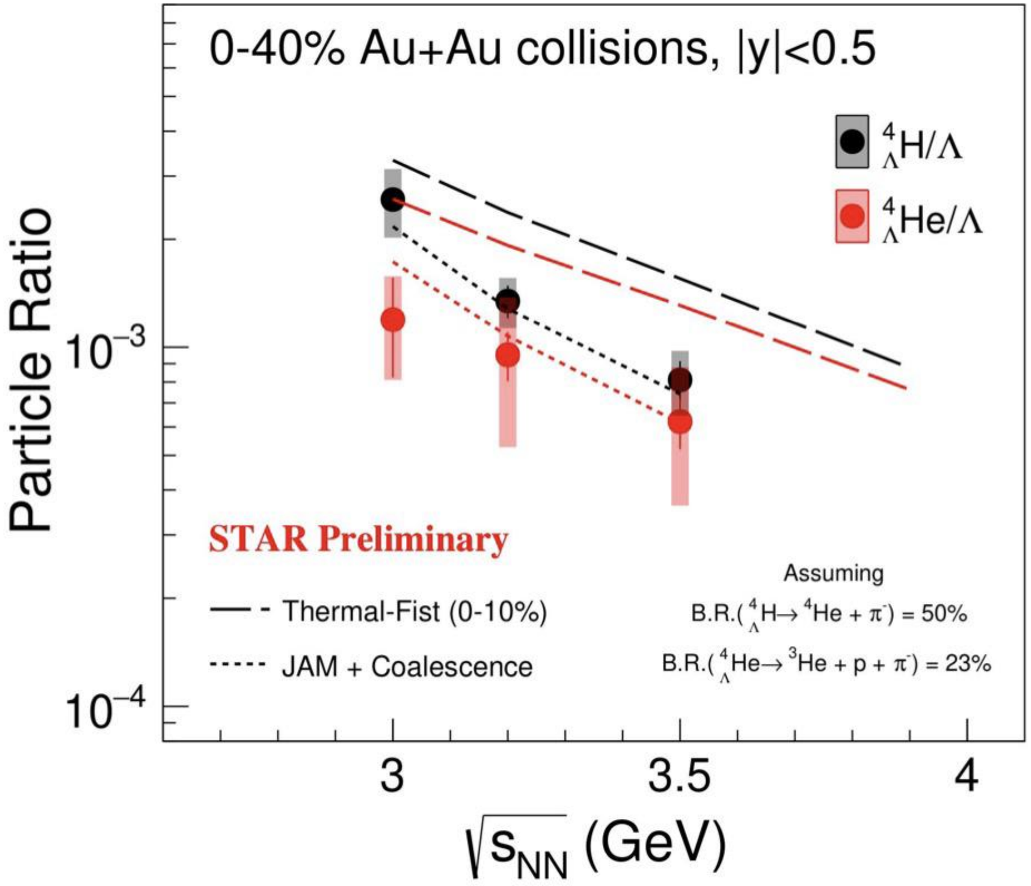

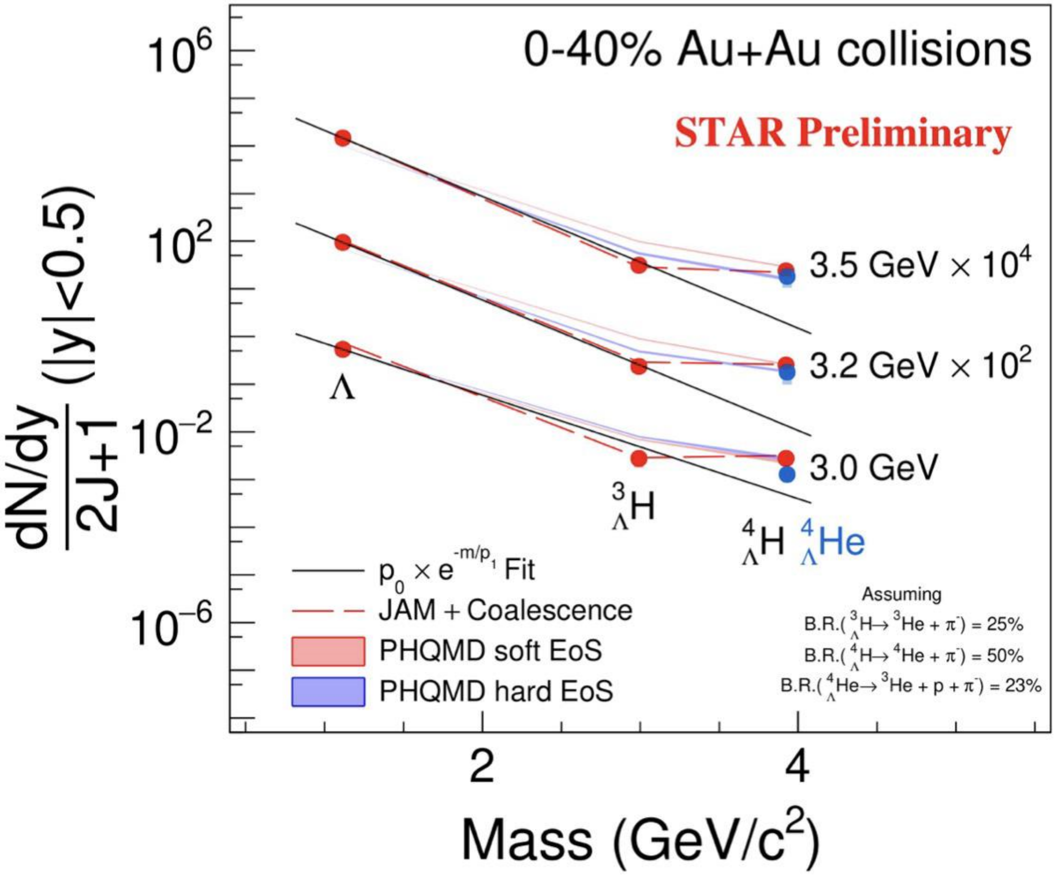

- Thermal model also over-predict A=4 hypernuclei yields while JAM+coal. describes the data.
- Enhanced ${}^{4}_{\Lambda}H$ production indicates a significant excited state feed-down contributions for A=4 hypernuclei. ${}^{4}_{\Lambda}H^*(J^+ = 1) \rightarrow {}^{4}_{\Lambda}H^*(J^+ = 0) + \gamma$

Strangeness Population Factor S_3 vs. $\sqrt{s_{NN}}$

Increasing trend of S_3 originally proposed as a signature of onset of deconfinement

$$S_3 = \frac{^3_\Lambda H}{^3He \times \frac{\Lambda}{p}}$$: removes the absolute difference of Λ/B yields versus beam energy.

- Data shows a hint of an increasing trend
- Coalescence + transport also suggest increasing trend – the energy dependence is sensitive to the source size, $^3_\Lambda H$ suppression due to large size

Phys. Rev. C 107 (2023) 1, 014912
Phys. Let. B 809 (2020) 135746

- Thermal-FIST also suggest increasing trend : unstable nuclei breakup $^4Li \rightarrow {}^3He\, p$

Phys. Lett. B 684 (2010) 224

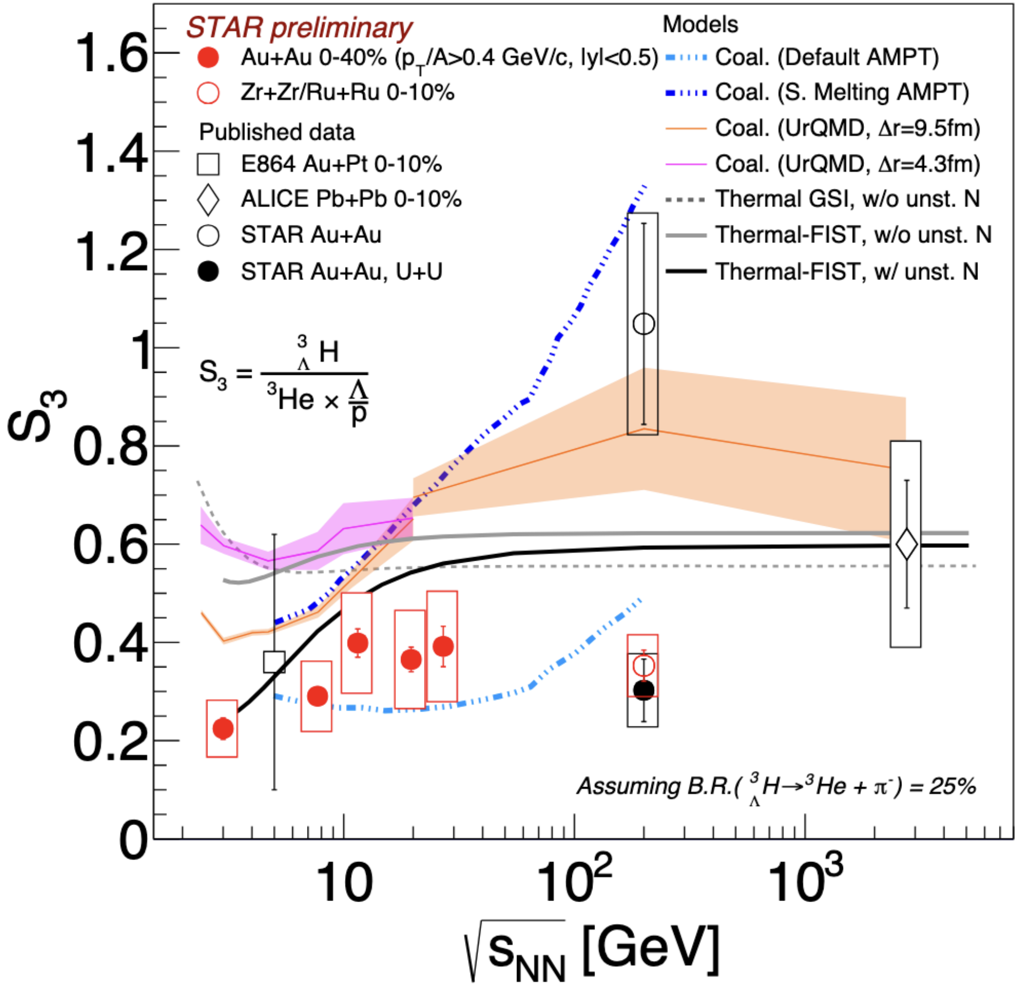

Provide constraints for hypernuclei production models in the high-baryon-density region

Note: For 19.6 and 27 GeV, take $^3He/t$ = 0.93±0.07

Energy Dependence of ${}^{3}_{\Lambda}H$ $\langle p_T \rangle$

- Similar $\langle p_T \rangle$ for ${}^{3}_{\Lambda}H$ and t
- Blast-wave fit using measured kinetic freeze-out parameters from light hadrons (π, K, p) overestimates both ${}^{3}_{\Lambda}H$ and t
- ${}^{3}_{\Lambda}H$ and t might do not follow the same collective expansion as light hadrons
- Different trend for $\sqrt{s_{NN}}$ =3-4.5 GeV and $\sqrt{s_{NN}}$ = 7.7-27 GeV

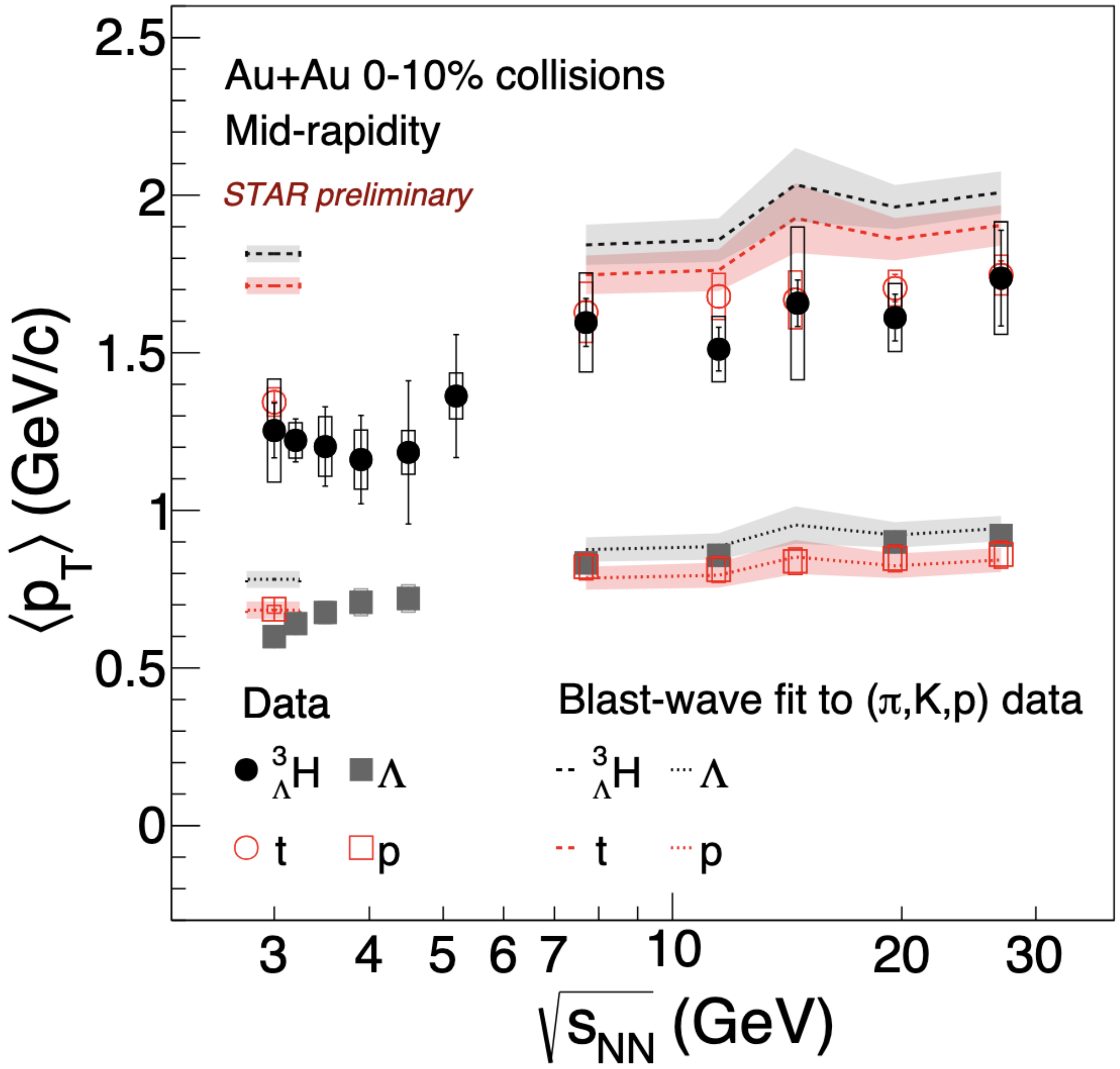

Suggest different expansion dynamics or medium properties?

Hypernuclei Collectivity vs. Mass

Phys. Rev. Lett. 130 (2023) 212301

$\langle p_T \rangle$ -> Radial flow contributions

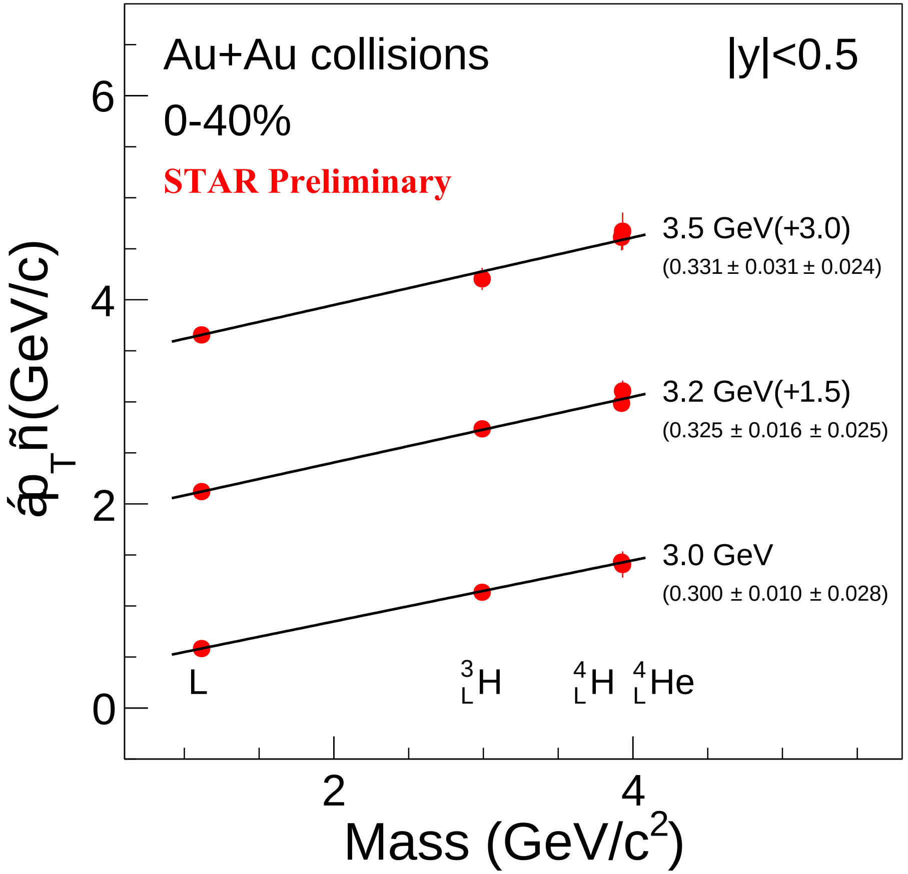

v_1 -> Directed flow

$$E\frac{d^3N}{dp^3} = \frac{1}{2\pi}\frac{d^2N}{p_T dp_T dy}\left(1 + \sum_{1}^{\infty} 2v_n \cos\left[n\left(\phi - \psi_{RP}\right)\right]\right)$$

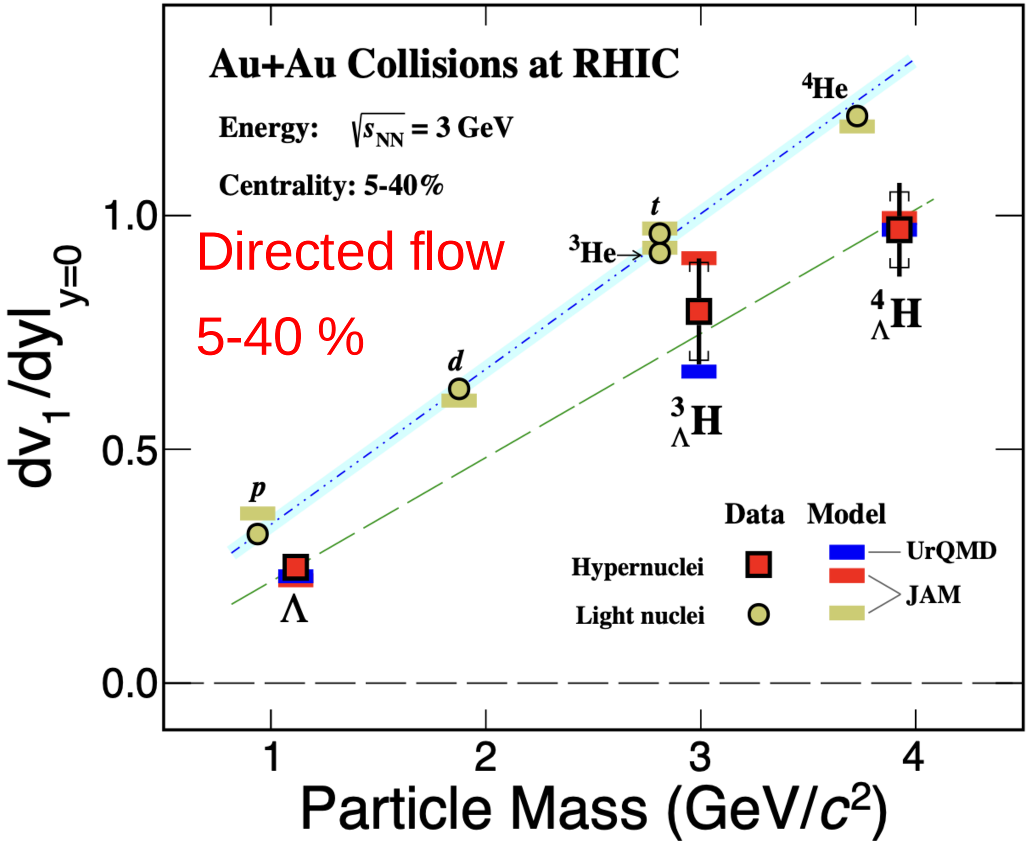

- Hypernuclei $\langle p_T \rangle$ (and v_1) show linear mass scaling from 3 to 3.5 GeV in mid-rapidity.
  - Consistent with coalescence formation picture.

Summary

- HyperNuclei Measurements @ STAR
  - ✓ Intrinsic Properties:
    -- Lifetime, Branch Ratios & Binding Energy
  - ✓ Productions and Collectivity:
    -- Energy Dependence

✓ Enhanced hypernuclei production at low energies allow precision measurement

✓ STAR data support coalescence mechanism of hypernuclei formation at mid-rapidity

✓ Thermal model over-predict A=3 (and A=4) hypernuclei yields

Outlook and Future Facilities

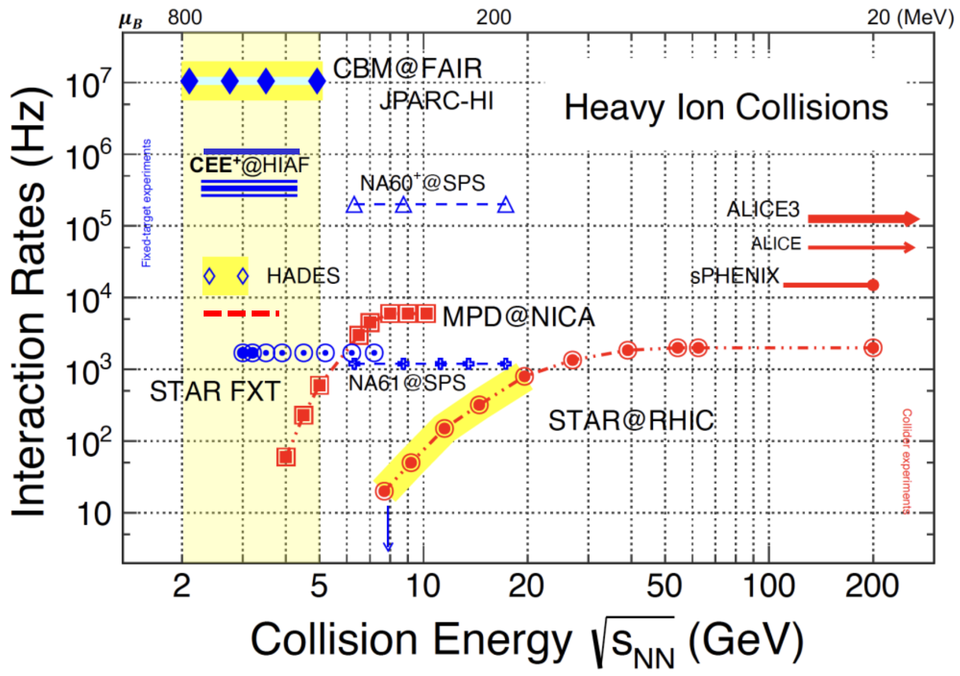

CEE+

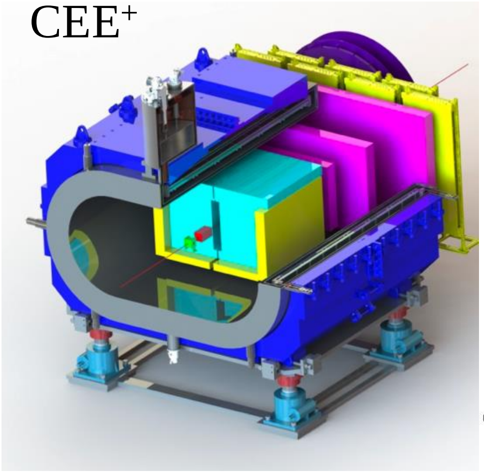

MPD

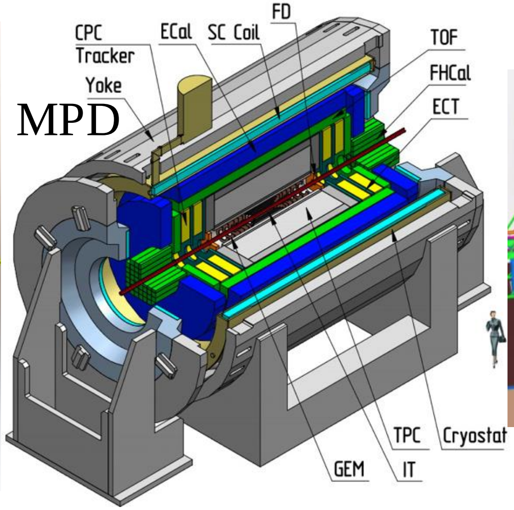

CBM

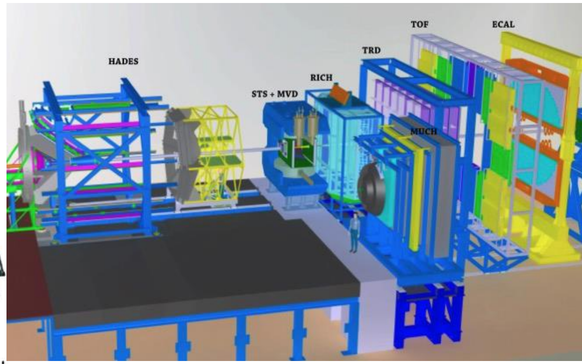

NICA/MPD 4-11 GeV, 2.4-3.5GeV FXT

FAIR/CBM 2-5 GeV

HIAF/CEE/CEE+ 2.2-4.5 GeV

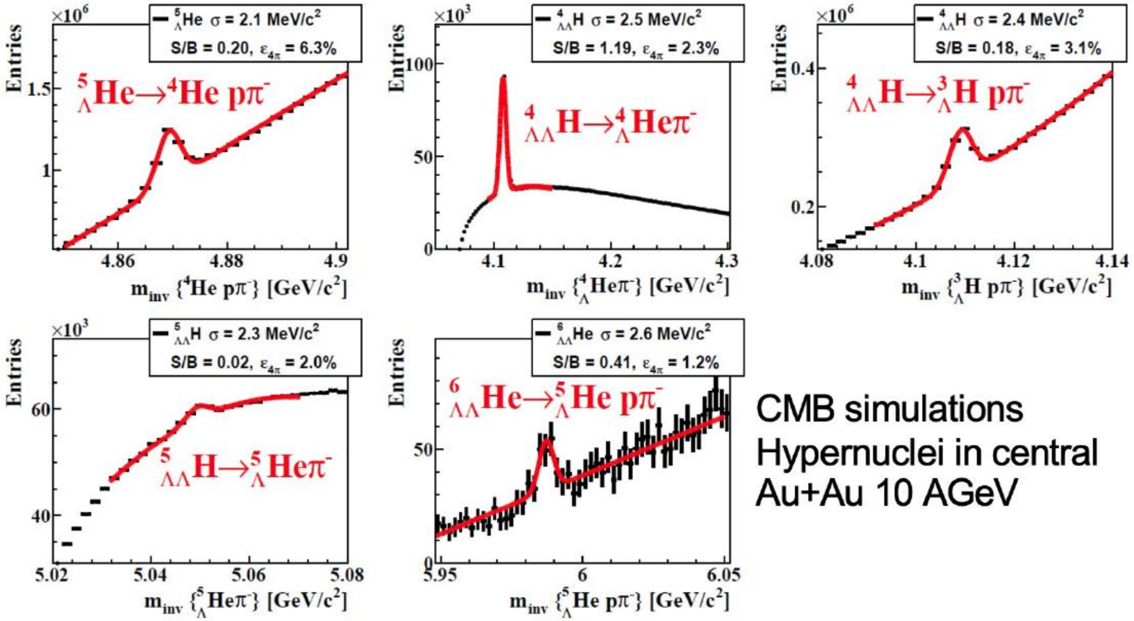

CMB simulations
Hypernuclei in central
Au+Au 10 AGeV

Perspectives

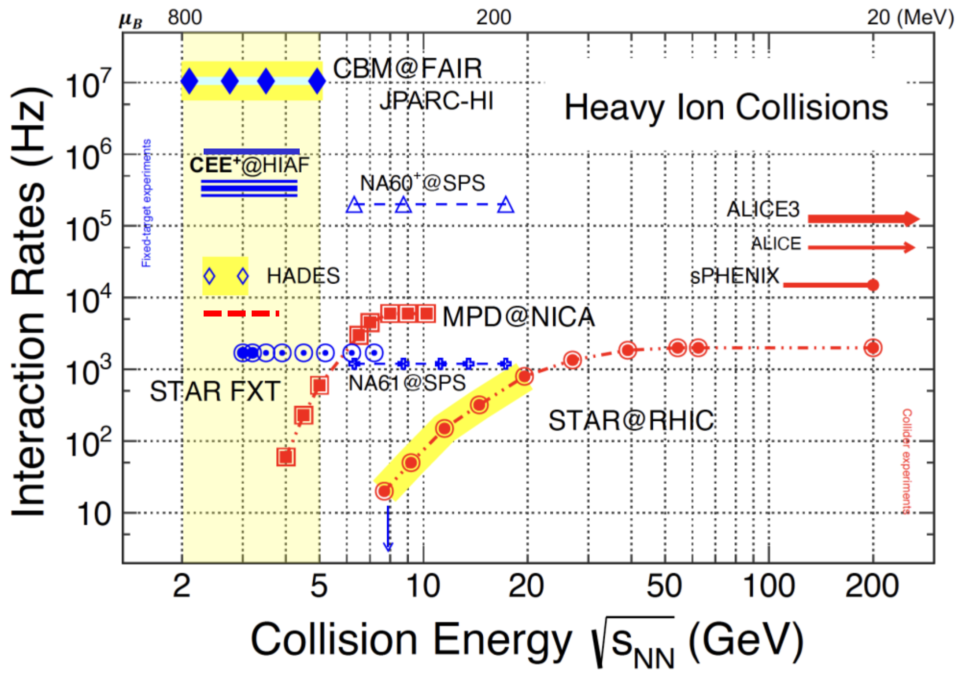

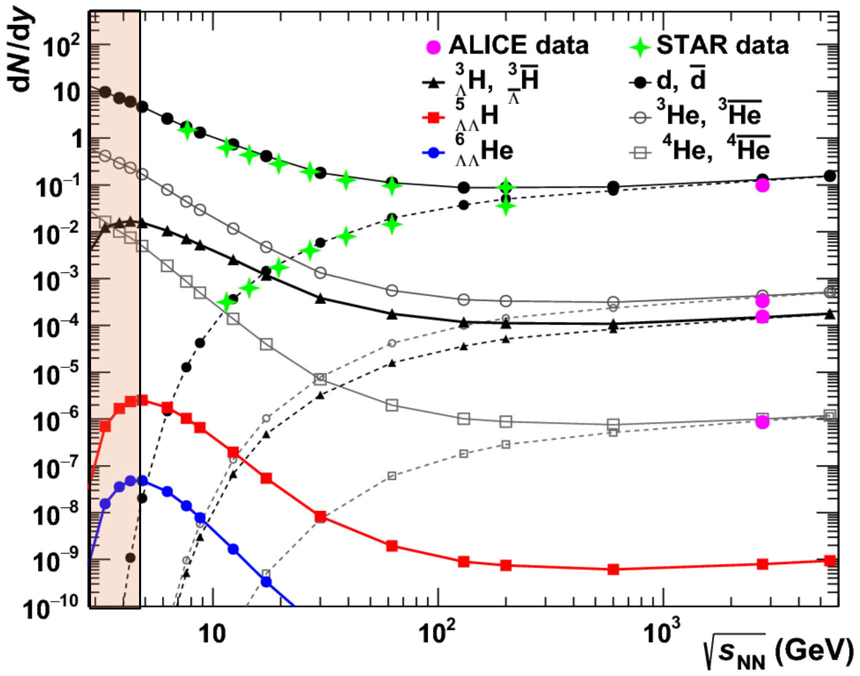

HIAF/CHNS 2.2-4.5 GeV: Biggest advantage & opportunity at this high baryon density region

- Precise measurements on the production/collectivity of A=3,4,5,6 hypernucleis (Λ, Σ, Ξ)
- (Double) Λ hypernuclei (YY): $^{4}_{\Lambda\Lambda}$H-> $^{4}_{\Lambda}$Heπ, $^{5}_{\Lambda\Lambda}$H -> $^{5}_{\Lambda}$Heπ, A=6 hypernuclei etc
- Direct correlation measurement: $p-\Lambda, d(t, He)-\Lambda, \Lambda-\Lambda, p-\Xi$ correlations.
- Precise measurements on the intrinsic properties
- Mirrored Particles with isospin dependence
- Hypernuclei Polarizations
- etc

中国科学院大学
University of Chinese Academy of Sciences

Thanks for Attention!

STAR Beam Energy Scan

Au+Au Collisions at RHIC											
Collider Runs						Fixed-Target Runs					
	$\sqrt{s_{NN}}$ (GeV)	#Events	μ_B	y_{beam}	run		$\sqrt{s_{NN}}$ (GeV)	#Events	μ_B	y_{beam}	run
1	200	380M	25MeV	5.3	r10,19	1	13.7(100)	50M	280MeV	-2.69	r21
2	62.4	46M	75MeV		r10	2	11.5(70)	50M	320MeV	-2.51	r21
3	54.4	1200M	85MeV		r17	3	9.2(44.5)	50M	370MeV	-2.28	r21
4	39	86M	112MeV		r10	4	7.7(31.2)	260M	420MeV	-2.1	r18,19,20
5	27	585M	156MeV	3.36	r11,18	5	7.2(26.5)	470M	440MeV	-2.02	r18,20
6	19.6	595M	206MeV	3.1	r11,19	6	6.2(19.5)	120M	490MeV	-1.87	r20
7	17.3	256M	230MeV		r21	7	5.2(13.5)	100M	540MeV	-1.68	r20
8	14.6	340M	262MeV		r14,19	8	4.5(9.8)	110M	590MeV	-1.52	r20
9	11.5	57M	316MeV		r10,20	9	3.9(7.3)	120M	633MeV	-1.37	r20
10	9.2	160M	372MeV		r10,20	10	3.5(5.75)	120M	670MeV	-1.2	r20
11	7.7	104M	420MeV		r21	11	3.2(4.59)	200M	699MeV	-1.13	r19
						12	3.0(3.85)	260+ 2000M	760MeV	-1.05	r18,20

Most Precise data to map the QCD phase diagram, $3 < \sqrt{s_{NN}} < 200\ GeV; 760 > \mu_B > 25\ MeV;$